energy&fuels

pubs.acs.org/EF

Review

# Review on Application of Nanotechnology for Asphaltene Adsorption, Crude Oil Demulsification, and Produced Water Treatment

Umer Farooq, Amit Patil, Balram Panjwani,* and Galina Simonsen

Cite This: *Energy Fuels* 2021, 35, 19191−19210

Read Online

ACCESS | Metrics & More | Article Recommendations

**ABSTRACT:** Nanotechnology is widely recognized for having important applications in many industries, one of which is oil and gas. Both environmental and cost benefits can be achieved when using nanoparticles for the separation of water and oil or further purification of produced water. More efficient emulsion separation can be achieved by selective adsorption of naturally present stabilizing components or magnetic action applied to nanoparticle-tagged droplets. The focus of this review is given to both nanoparticles and nanocomposites that have been studied with respect to asphaltene adsorption, crude oil demulsification, and produced water treatment, as well as oil spill cleanup and improvement of antifouling resistance of filtration membranes. Asphaltene chemistry and its role in emulsion stabilization are discussed in detail.

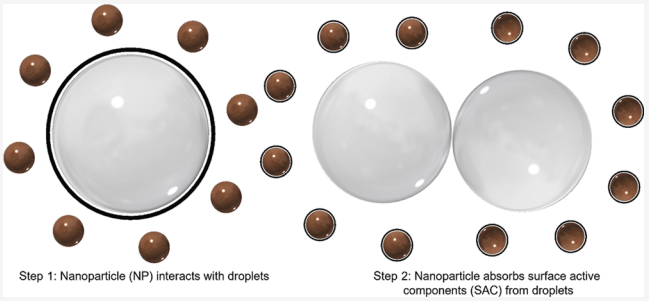




## 1. INTRODUCTION

Naturally present surface-active molecules, such as asphaltenes, are commonly found in crude oils all around the world. Asphaltenes are a broad class of high-molecular-weight hydrocarbon substances that are soluble in light aromatic compounds, such as benzene or toluene, and are insoluble in low-molecular-weight compounds, like pentane and heptane.[1−3] The asphaltenes are considered to be some of the main contributors to a range of flow assurance- and process-related problems leading to enormous financial losses for the petroleum industry.[4] One reported example is from an oil field in the Gulf of Mexico where the cost of a well shut-in for cleanup operation due to asphaltene deposition was estimated at approximately $70 million/well.[5] Complications related to asphaltene contribution to the crude oil emulsion stability can affect several operations in the production chain from a reservoir to oil storage. Already at the well, the presence of a high amount of asphaltenes can cause reduced oil recovery through altering the reservoir properties such as wettability and plugging of the rock pores,[6−8] as well as the formation of solid deposits within the wells.[9] The presence of the destabilized asphaltenes may lead to major pipelines and wellbore blockages,[10] formation and stabilization of emulsions, adsorption onto process equipment,[11] plugging while oils are stored, fouling and corrosion of production equipment, catalyst deactivation,[12,13] and coke formation.[14,15]

Asphaltenes can also be defined by a large number of aromatic rings with a hydrogen/carbon (H/C) ratio of 1.15 ± 0.05%.[16] Depending on the crude oil source,[17] the molecular weight of asphaltene molecules ranges from 250 to 1200 g/mol.[18,19] The proposed molecular structure of asphaltenes possesses coexisting island and archipelago motifs of asphaltene monomers.[20−22] The asphaltene fractions also contain the largest percentage of heteroatoms (oxygen (O), sulfur (S), nitrogen (N)) and traces of organometallic constitutents.[23] Generally, the S atoms (0.3%−10.3%) are present in heterocycles, sulfide, or thiophene groups. N (0.6%−3.3%) may be present as pyrrolic, pyridine, and quinoline types of functional groups, and O (0.3%−4.9%) can be present as hydroxyl, carbonyl, and carboxyl groups.[24] It is important to mention that O- and N-containing groups impart positive and negative charges, respectively. Typically, pyridine is identified as the major contributor to the basicity of asphaltenes, whereas carboxylic acid groups are the main contributors toward acidity of asphaltenes.[25,26] The organometallic complexes mostly contain vanadium(V),[27,28] nickel (Ni), and iron (Fe).[29] These metal complexes, particularly porphyrins, are excessively found in asphaltene deposits and are known as major contributors to fouling in pipelines.[29]

**Received:** June 18, 2021
**Revised:** October 20, 2021
**Published:** November 18, 2021

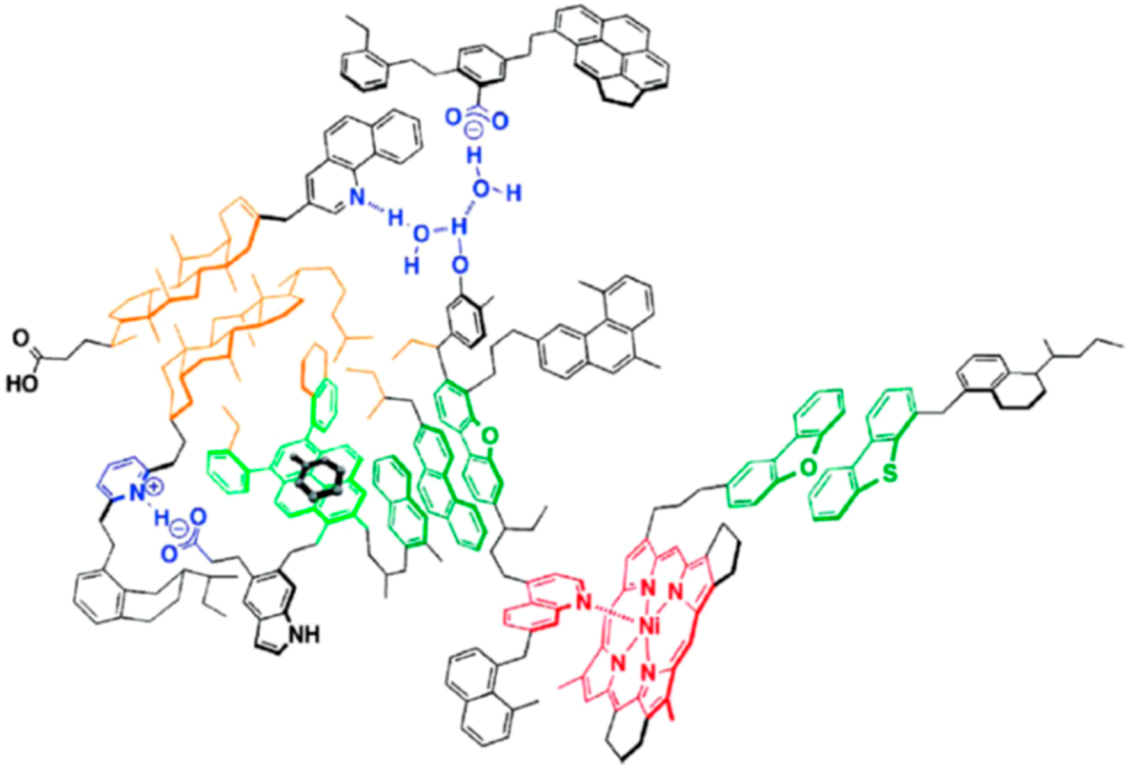


**Figure 1.** Proposed supramolecular assembly of asphaltenes showing different association mechanisms in different colors: blue, acid−base and hydrogen bonding interactions; red, metal coordination complex; orange, hydrophobic pocket; and green, $\pi-\pi$ stacking interactions.[37]

The polycyclic aromatic sheets of asphaltenes comprise polarizable groups, i.e., heteroatoms possessing a degree of charge. This activates the dipole−induced dipole and dipole−dipole attractive interactions or so-called stacking propensity.[30] On the other hand, for preventing the close molecular approach, steric hindrance occurs in the peripheral substituents of asphaltenes. Consequently, to maintain a balance between the stacking propensity and its hindrance, the aggregation predisposition is produced in asphaltenes. Depending on the crude oil composition and reservoir conditions, the asphaltene self-association in reservoir oil samples causes the formation of 5−20 nm asphaltene aggregates. Temperature, pressure, and composition changes are inherent during oil production. This causes aggregates to destabilize, forming 6−300 nm-sized nanoaggregate clusters.[31] If the asphaltene instability proceeds further, then the cluster size may increase and form 500−1000 nm flocs. Thus, the flocs can overcome the Brownian forces in suspension causing asphaltene precipitation out of the liquid phase.[32]

Resins are also another type of polar crude oil component having a profound influence on the stability behavior of asphaltenes in crude oils as they can prevent the separation of the asphaltene molecules. In terms of structure, resins are very similar to asphaltenes; however, they have a lower molecular weight (MW) (<1000 g/mol) and higher hydrogen/carbon (H/C) ratio (1.2−1.7).[33,34] Moreover, as compared to asphaltenes, resins have smaller chromophores and relatively longer aliphatic side chains, which increase their solubility in aliphatic solvents.[35] The molecular interaction between asphaltenes and resins and their ratio with respect to other components in crude oils are vital for the stabilization of crude oil emulsions. Resins act as a link between the nonpolar saturates and polar asphaltenes of the crude oil through various suggested mechanisms, i.e., micelle-type formation,[29] peptization of asphaltene core,[36] or as supramolecular growth.[37]

Asphaltenes are most commonly precipitated from light crude oils containing a low fraction of asphaltenes. The reason for this is that the alkanes, which are generally present in large amounts in the light crude oils, have less solubility for asphaltenes. On the contrary, asphaltene-rich heavy crude oils contain large amounts of intermediate compounds, which are effective solvents for asphaltenes. However, it is also a fact that during downstream operations heavy oils can contribute to the earlier mentioned challenges, leading to coking, fouling, and catalyst deactivation during processing or upgrading.[38,39]

Various intermolecular forces can enhance the process of asphaltene surface adsorption, such as acid−base interaction, hydrogen bonding (H-bonding) (more pronounced in the presence of water), van der Waals forces, coordination complexes, and $\pi-\pi$ stacking are present[37] (Figure 1). Asphaltene adsorption is a practically and industrially accepted strategy for asphaltene elimination and is dependent on various factors, which makes it highly complex process. Typical sorbents can be divided into mineral based (clay and rock minerals), silica, alumina, glass, carbon, metals, metal oxides, and polymers.[40] Interest in metal oxide nanoparticles has also been growing as nanomaterials offer exceptionally large and functional surface areas that exhibit an appropriate surface activity and selectivity toward asphaltene molecules.[41]

During the production and transportation of crude oils, due to the presence of saline water, it has often happened that very stable and complex emulsions are formed.[42−44] These oil−water emulsions are stabilized by particles, production chemicals, and indigenous surface-active compounds. Among all indigenous compounds, asphaltenes are thought to play the dominant role during emulsion formation. The formed


https://doi.org/10.1021/acs.energyfuels.1c01990
Energy Fuels 2021, 35, 19191−19210

emulsions consist of complex colloidal structures, and the two combined liquid phases are mutually immiscible.[45] Crude oil emulsions typically occur when oil and water are vigorously stirred during production.[46,47] On the basis of the nature of the dispersed phase, emulsions can be classified into two main types: oil droplets in water refer to O/W emulsions, and water droplets in oil refer to W/O emulsion. There are also multiple emulsion types, such as oil-in-water-in-oil (O/W/O) and water-in-oil-in-water (W/O/W)[48] as shown in Figure 2.

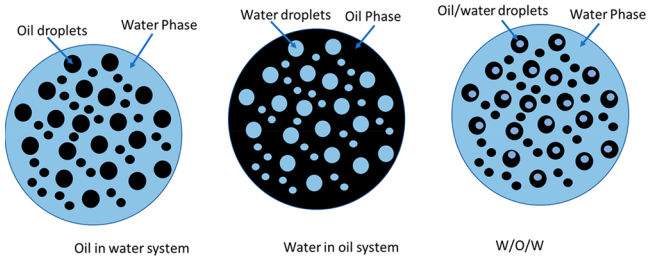


**Figure 2.** Different types of emulsions found in crude oil production and transport.

The natural stabilizing components present in the crude oils include asphaltenes, resins, and acidic compounds (e.g., naphthenic, fatty, and aromatic acids) play an important combined role in emulsion formation and stability.[45] Kilpatrick[49] found that 7−20 nm asphaltene aggregates are responsible for the stabilization of interfacial films formed at the interfaces between droplets in crude oil emulsions. Moreover, Fan et al.[50] revealed that emulsion stabilization was greatly enhanced by asphaltene aggregation and concentration. Similar to the asphaltenes, resins consist of multiple macromolecular nonhydrocarbon compounds and play an important role in the overall emulsion stability.[33] Unlike asphaltenes, the emulsion stabilized solely by resins has reduced stability due to the lower thickness of the formed interfacial films.[51] However, it is also widely recognized that asphaltenes and resins act synergistically. According to Kar and Hascakir,[33] the stability of emulsion formed by asphaltenes is weaker on the addition of the resins. On the other hand, removal of asphaltenes or reduction of their content will change the overall ratio between asphaltenes and resins and will also contribute to reduced emulsion stability.

To avoid financial losses and operational challenges before oil transport to refineries, there is a requirement to separate oil−water emulsion into two discrete phases.[52] The separation process, also known as demulsification, is often achieved by selecting the suitable demulsifier.[53−55] Several demulsification strategies have been reported in the literature,[56−58] and these can be divided into three major groups, namely, biological, chemical (demulsifiers), and physical (electrical, mechanical, thermal, ultrasonic, and membrane) demulsification processes.[52] Among these methods, chemical demulsification has been extensively tested and discussed in the literature.[59−61] The main function of the chemical demulsifiers is to disrupt the interfacial films between emulsion droplets and weaken the effect of surface-active agents.[62] The mechanism is based on alteration of IFT, surface elasticity, mechanical strength, and thickness of the interfacial films, leading to higher droplet flocculation rates and/or coalescence. Although chemical demulsification is one of the widely used approaches for breaking stable emulsions, those demulsifiers are environmentally unfriendly, corrosive, and toxic. Moreover, separated water must be processed to remove traces of harmful organic polymers prior to being released into environment.

Produced water is water coproduced during crude oil production and processing. Pollutants like dispersed oil droplets, dissolved components, and solids must be separated from the produced water prior to its discharge or reinjection. Release of the produced water is one of the major environmental concerns related to the oil exploration and calls for efficient treatment processes to remove of a variety of polluting components. Several technologies are currently employed to remove pollutants from produced water. This includes gravity oil separators, coalescers, and chemical oxidation. But all conventional technologies have certain complications and limitations, and due to more stringent regulations and quality standards, it is difficult to meet the requirements. Moreover, due to platform space constraints, a compact treatment technology is required.[63−65]

Nanoparticles (NPs) or nanoscale particles represent a number of unique properties, such as extremely large surface area and possibilities for surface functionalization. They offer variable performance dependent on composition, synthesis method, dimensions, and surface structures. Physico-chemical affinity of the NPs toward specific surfaces results in a variety of applications, one of which is selective adsorption of unwanted components from liquid streams. NPs with a surface affinity toward asphaltenes and the capability of positioning themselves at the oil−water interface can be used for effective demulsification of stable crude oil emulsions. Another approach is a permanent attachment of the functional NPs onto a supporting matrix, so-called nanocomposites. In comparison with NPs, nanocomposites exhibit higher mechanical stability, process ability, and some advantages caused by the NP−matrix interactions. Moreover, magnetic NPs can also enhance the demulsification process by adsorbing at the surfaces of emulsion droplets.[66,67] After application of an external magnetic field, these droplets accumulate, coalesce, and subsequently separate. The interfacial activity, which is one of the most prominent properties of the NPs, is typically introduced by functionalization reactions design to introduce specific functional groups.

The objective of this comprehensive literature review is to investigate the potential of nanomaterials, both NPs and nanocomposites, for asphaltene adsorption, crude oil demulsification, and produced water treatment. Focus is given to the assessment of some recent developments on the experimental front and identification of the knowledge gaps illustrating overall trends to invigorate future research. It is important to mention that comparing existing studies is not straightforward as researchers use different approaches, methods, materials, conditions, and solvents. Therefore, many inconsistences are found throughout literature. For instance, in model or synthetic oil solutions (asphaltene/solvent mixtures), the extent of asphaltene aggregation is concentration dependent,[68] so higher adsorption can be achieved from more aggregated oils than from less aggregated oil solutions.[69] Moreover, the asphaltene-containing liquid medium is crucial as high polarity solvents can disperse the aggregates or compete for adsorption, i.e., ratios of heptane−toluene (Heptol) are important for adsorption experiments as Heptol solutions enhance the aggregation degree at decreasing solvent strength.[70,71] In some cases, adsorption methods lead to different results; i.e., a batch adsorption experiment can be performed in two different


https://doi.org/10.1021/acs.energyfuels.1c01990
Energy Fuels 2021, 35, 19191−19210

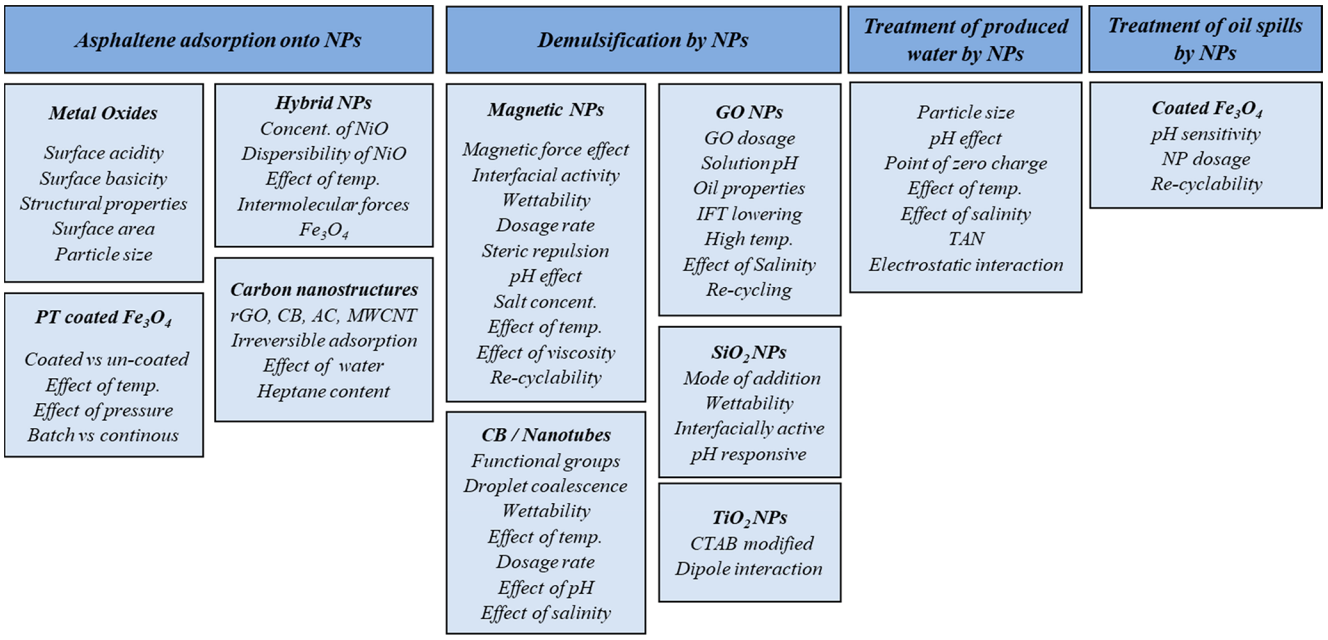


**Figure 3.** General sketch of review article.

ways: (1) exposing a certain mass of NPs under variable asphaltene concentration and (2) exposing a given asphaltene concentration while varying the NP dosage.[72] The source and MW are also important as they affect asphaltene adsorption rate, affinity, and capacity.[73] Moreover, the methodology for asphaltene isolation from the crude oils has to be taken into consideration, as C7-extracted asphaltenes show higher polarity and aromaticity than the C5 extracted asphaltenes.[74] The above-mentioned effects and others, such as the chemical and physical properties of the NPs, composition of the asphaltenes, temperature, pressure, and water content, are discussed in detail in the next sections. The general sketch of this review is summarized in Figure 3.

## 2. ASPHALTENE ADSORPTION ONTO NANOPARTICLES

In this section, asphaltene adsorption onto NPs studied by different authors is discussed and summarized in Table 1. Four categories of NPs (pure metal oxides, hybrid NPs, carbonaceous nanostructures, and surface-coated NPs) have been considered. The hybrid NPs are developed by combining at least two different NPs to overcome the limits with single NPs and to achieve new tailored properties. The coated NPs can be synthesized by coating each individual NP with a second ceramic or polymer layer (e.g., polythiophene (PT)).

**2.1. Metal Oxides.** There are several factors and mechanisms that govern asphaltene adsorption onto metal oxide surfaces. These mechanisms are presented in Figure 4 and described in the sections below.

*2.1.1. Surface Acidity and Basicity.* The surface acidity and basicity impacts of metal oxide NPs on asphaltene adsorption were investigated by several authors[41,74−80] who concluded that the extent of acid−base interactions and electrostatic attractions may be the main adsorption mechanisms. It has been previously suggested that the basic components in crude oils were mostly present in the form of asphaltene fractions.[81] Therefore, metal oxides with the highest density of surface acidic sites demonstrated the greatest capacity and affinity toward asphaltenes. Among different types of metal oxides/salts used for adsorption studies of asphaltenes, it was reported that the adsorption capacity of NPs was decreased as follows: NiO > $Fe_2O_3$ > $WO_3$ > MgO > $CaCO_3$ > $ZrO_2$. This was associated with the synergetic effects of the surface acidity as well as the total net charge of the NP surfaces.[41] Similar effects were found in a study where all tested NPs showed higher adsorption affinity (12.4−63.3 mg/m$^2$) toward asphaltenes in the order of NiO > $Co_3O_4$ > $Fe_3O_4$.[75] However, another study also suggested that the adsorption affinity ($K_L$, Langmuir equilibrium adsorption constant) does not correlate with the adsorption capacity ($Q_{max}$).[74] Nassar et al. selected six different types of commercially available metal oxide NPs and found that the $Q_{max}$ of the oxides decreased as follows: CaO > $Co_3O_4$ > $Fe_3O_4$ > MgO > NiO > $TiO_2$, whereas $K_L$ had the following order: NiO > $TiO_2$ > CaO> $Co_3O_4$ > $Fe_3O_4$ > MgO. Their results revealed that the adsorption extent and adsorption quality were not always related, and the acidic natures of the NPs were important for the adsorption capacities as basic oxides (CaO and MgO) and amphiprotic oxides ($Fe_3O_4$ and $Co_3O_4$) showed greater adsorption capacities than the acidic oxides (NiO and $TiO_2$). On the contrary, the adsorption qualities measured by the $K_L$ values were greater for the acidic oxides (NiO and $TiO_2$).[74]

Later, Betancur et al.[76] tailored $SiO_2$ NPs by acid, base, and neutral treatments, and the effects of surface properties of the NPs on the adsorption of asphaltenes from Heptol solutions were estimated. The results revealed that NPs with the highest total acidity had the highest adsorptive capacities for n-C7 asphaltenes. In addition to that, the amount of adsorbed n-C7 asphaltenes was found to correlate with the surface acidity. At the same time, the basic and neutral functionalizations had no influence on the NP adsorptive capacity.[76] Similar results were reported in another study, where acidic $SiO_2$ NPs showed higher adsorption than $SiO_2$ and $Al_2O_3$ NPs.[77] Moreover, the acidic nature of the zeolite beta BEA-NPs were also found effective in adsorbing asphaltenes from a toluene solution.[80] Synthesized maghemite ($\gamma$-$Fe_2O_3$) NPs also showed higher


https://doi.org/10.1021/acs.energyfuels.1c01990
Energy Fuels 2021, 35, 19191−19210

**Table 1. Summary of Asphaltenes Adsorption onto Nanoparticles (NPs)**

| Types of NPs | Experimental conditions | $Q_{max}$ mg/m$^2$ | $K_L$ (L/mg) | Ads. amount asphaltenes (mg/g) | ref |
|---|---|---|---|---|---|
| NiO | 100−3000 mg/L (asphaltenes in toluene); NPs dosage, 5 g/L; equilibrium (eq) time, 24 h | 3.67 | 0.0131 | | 41 |
| $Fe_2O_3$ | | 3.52 | 0.0144 | | |
| $WO_3$ | | 3.35 | 0.0090 | | |
| MgO | | 2.62 | 0.0155 | | |
| $CaCO_3$ | | 2.17 | 0.0158 | | |
| $ZrO_2$ | | 1.23 | 0.0106 | | |
| NiO | 150−3000 mg/L (asphaltenes in toluene); NPs dosage, 10 g/L at 25 °C | 0.58 | 0.016 | | 74 |
| $Fe_3O_4$ | | 1.7 | 0.005 | | |
| $Co_3O_4$ | | 1.76 | 0.008 | | |
| MgO | | 1.35 | 0.004 | | |
| CaO | | 2.7 | 0.008 | | |
| $TiO_2$ | | 0.54 | 0.009 | | |
| NiO | 200−2000 mg/L (asphaltenes in toluene); NPs dosage, 10 g/L at 25 °C; eq time, 24 h | | | 22.3−60.1 | 75 |
| $Co_3O_4$ | | | | 12.4−63.3 | |
| $Fe_3O_4$ | | | | 15.1−62.0 | |
| $ZrO_2$ | 300−2000 mg/L asphaltenes in toluene; NPs dosage, 10 g/L at 25 °C; eq time, 24 h | 1.7−2.8 | | | 89 |
| $CeO_2$ | | 1.5−2.3 | | | |
| $TiO_2$ | | 0.4−0.5 | | | |
| $SiO_2$ | 100−1000 mg/L asphaltenes in toluene; NPs dosage, 10 g/L at 25 °C | | | 8−90 | 84 |
| MgO | | | | 8−55 | |
| $Al_2O_3$ | | | | 1−10 | |
| $SiO_2$ - A | 100−1500 mg/L asphaltenes in Heptol; NPs dosage 10 g/L | | | 50−500 | 77 |
| $SiO_2$ | | | | 30−300 | |
| $Al_2O_3$ | | | | 10−70 | |
| In situ NiO | 40000 mg/L asphaltenes in toluene; NP dosage, 15 g/L at 25 °C; eq time, 2 h | | | 2690 | 87 |
| Comm. NiO | | | | 420 | |
| Magnetite | 10−10,000 mg/L asphaltenes in toluene; NP dosage, 13 g/L at 25 °C; eq time, 90 min | | | 5−500 | 82 |
| In situ $Fe_2O_3$ | 10000−40,000 mg/L asphaltenes in toluene; NP dosage, 1−10 g/L at 25 °C; eq time, 1 h | | | 2600 ± 120 | 88 |
| Comm. $Fe_2O_3$ | | | | 600 ± 200 | |
| $\gamma$-$Fe_2O_3$ | 100−1000 mg/L asphaltenes in toluene; NP dosage, 10 g/L at 25 °C; eq time, 2 h | | | 9−56 | 79 |
| $\gamma$-$Fe_2O_3$ | 100−1000 mg/L asphaltenes in toluene; NP dosage, 5−10 g/L at 25 °C; eq time, 1 h | | | 9−56 | 78 |
| $\alpha$-$Fe_2O_3$ | | | | 8−30 | |
| Nanosilica | 100−30,000 mg/L asphaltenes in toluene; NP dosage, 10 g/L at 25 °C | | | 100−1000 | 86 |
| $\mu$-Silica | | | | 30−330 | |
| $SiO_2$ | 2000 mg/L asphaltenes in toluene; NP dosage, 30 g/L at 40 °C; eq time, 40 h | | | | 71 |
| $SiO_2$ cellulose | | | | | |
| $SiO_2$ PEG | | | | | |
| $SiO_2$ chitosan | | | | | |
| Silica gel-acid | 1000 mg/L asphaltenes in Heptol 60; NP dosage, 10 g/L at 25 °C; eq time, 20 min | | | 58 | 76 |
| Silica gel-base | | | | 48 | |
| Silica gel-neutral | | | | 49 | |
| Silica gel | | | | 42 | |
| $\gamma$-$Al_2O_3$ | 100−1000 mg/L asphaltenes in Heptol; NP dosage, 10 g/L at 25 °C; eq time, 2 h | | | 7.5−70 | 68 |
| Nano-$Al_2O_3$ | 100−3000 mg/L asphaltenes in toluene; NP dosage, 10 g/L | 0−1.7 | | | 85 |



https://doi.org/10.1021/acs.energyfuels.1c01990
Energy Fuels 2021, 35, 19191−19210

**Table 1. continued**

| Types of NPs | Experimental conditions | $Q_{max}$ mg/m$^2$ | $K_L$ (L/mg) | Ads. amount asphaltenes (mg/g) | ref |
|---|---|---|---|---|---|
| $\mu$-$Al_2O_3$ | | 0−0.4 | | | |
| Silica | 150−750 mg/L asphaltenes in toluene; NP dosage, 10 g/L at 25 °C; eq time: 2 h | | | 10−60 | 95 |
| SiNi5 (Ni 5%) | | | | 15−150 | |
| SiNi15 (Ni 15%) | | | | 15−160 | |
| AlNi15 | 150−1500 mg/L asphaltenes in toluene; NP dosage, 10 g/L at 25 °C; eq time, 2 min | 2.0−9.0 | | | 96 |
| SNi15 | | 0.5−5.5 | | | |
| SNi5 | | 0.2−4 | | | |
| AlNi5 | | 0.2−2 | | | |
| Silica gel (amorphous) | | 0.1−0.8 | | | |
| Alumina | | 0.1−0.7 | | | |
| Fumed silia gel | | 0.1−2.1 | | | |
| Silica (crystalline) | | 0.1−2 | | | |
| Silica gel (commercial) | | 0.1−2 | | | |
| Alumina I | | 0.1−0.5 | | | |
| Zeolite | | 0.1−0.5 | | | |
| PdNi/Al | | 0.1−0.4 | | | |
| Washed rock | | 0.1−0.3 | | | |
| Unwashed rock | | 0.2−2 | | | |
| $Fe_3O_4$ | 100−1500 mg/L asphaltenes in toluene; NP dosage, 5 g/L at 25 °C | | | 10−65 | 99 |
| $Fe_3O_4$@CHI | | | | 10−75 | |
| $Fe_3O_4$@$SiO_2$ | | | | 10−50 | |
| Chitosan | | | | 3−25 | |
| $SiO_2$ | | | | 3−30 | |
| AC | 200−3000 mg/L asphaltenes in 37 vol % Heptol; NP dosage, 2 g/L at 30 °C; eq time, 1 − 24 h | | | 10−110 | 70 |
| CB | | | | 150−280 | |
| MWCNT | | | | 100−560 | |
| rGO | | | | 250−700 | |
| $Fe_3O_4$ | 100−1000 mg/L asphaltenes in toluene; NP dosage, 2−20 g/L at 25 °C; eq time, 2 h | 2−14 | | | 101 |
| $Fe_3O_4$-PT | | 3−19 | | | |
| $Fe_3O_4$ | | 0.095−3 | | | |
| $Fe_3O_4$-PT | | 0.1−4.1 | | | |
| $Fe_3O_4$ | NP dosage, 10 g/L at 25 °C; eq time, 2 h | 3.79 (B) | | | 102 |
| $Fe_3O_4$-PT | | 3.31 (C) | | | |
| $Fe_3O_4$-MOF | | 4.96 (B) | | | |
| $Fe_3O_4$-GO | | 4.51 (C) | | | |
| $Fe_3O_4$-$SiO_2$ | | 4.75 (B) | | | |
| $Fe_3O_4$-chitosan | | 4.15 (C) | | | |
| | | 4.52 (B) | | | |
| | | 4.01 (C) | | | |
| | | 3.75 (B) | | | |
| | | 3.26 (C) | | | |
| | | 4.11 (B) | | | |
| | | 3.61 (C) | | | |
| Zeolite beta | 100−3000 mg/L asphaltenes in toluene; NP dosage, 10 g/L | 0.1−1.98 | | | 80 |

adsorption affinity toward asphaltenes than hematite ($\alpha$-$Fe_2O_3$) NPs due to their surface acidity.[78,79]

*2.1.2. Surface Area, Particle Size, and Initial NP Concentrations.* Variations in the adsorption affinities, capacities, and kinetics of the metal oxide NPs are attributed to the surface area and abundance of active sites available for adsorption.[78,80,82−84] It was demonstrated that NiO NPs exhibit greater adsorption affinity than $Fe_3O_4$ and $Co_3O_4$ NPs. This was attributed to larger surface areas of the NiO NPs compared to $Fe_3O_4$ and $Co_3O_4$ NPs.[83] Similar results were reported for $SiO_2$ NPs, which showed higher adsorption affinity toward asphaltenes than MgO and $Al_2O_3$ because of larger surface areas (adsorption efficiency was in the order of $SiO_2$ > MgO > $Al_2O_3$[84]). The smallest mean particle size and high surface area were also responsible for strong adsorption of asphaltenes from a Heptol solution onto the modified acidic


https://doi.org/10.1021/acs.energyfuels.1c01990
Energy Fuels 2021, 35, 19191−19210

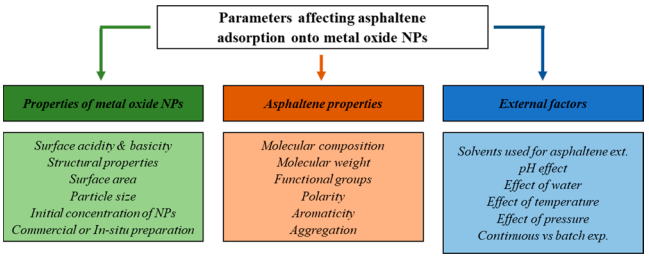


**Figure 4.** Parameters affecting asphaltene adsorption onto metal oxide NPs.

$SiO_2$ NPs.[76] In another study, Al-Jabari et al used 20−30 nm $Fe_3O_4$ NPs for asphaltene removal from a toluene solution[82] and found that removal of asphaltenes increased as the higher amounts of NPs were added to the solution. The adsorption equilibrium was reached within 90 min (80% of the asphaltenes were removed).[82] Moreover, the higher adsorption affinity of asphaltenes toward $\gamma$-$Fe_2O_3$ NPs was also attributed to their higher surface area than that of the $\alpha$-$Fe_2O_3$ NPs.[78] Nassar et al. also explored the adsorption of two $Al_2O_3$ with similar acidity but different particle sizes. The results revealed that on a surface area basis, nano-$Al_2O_3$ (<50 nm) had greater adsorption capacity than micro-$Al_2O_3$ (50−200 $\mu$m).[85] A study also revealed that nanosilica ($SiO_2$) showed almost 10 times higher n-C7 asphaltene adsorption than microsilica particles due to their high dispersibility and available exposed adsorption surface area.[86]

*2.1.3. Commercial vs In Situ-Prepared NPs.* The in situ-prepared NPs interacted better with asphaltenes due to their effective dispersion in the solution. The less effective dispersion of commercial NPs potentially reduced their total surface area and established internal and external mass transfer limitations.[87,88] In one of the studies, it was observed that the commercial NiO NPs of the same size range adsorbed 85% less than the in situ-prepared NiO under the same experimental conditions.[87] Moreover, the same authors demonstrated that the in situ $Fe_2O_3$ NPs displayed higher adsorption (2.6 ± 0.12 g asphaltenes/g NPs) compared to the commercial $Fe_2O_3$NPs (0.6 ± 0.2 g asphaltenes/g NPs).[88]

*2.1.4. Asphaltene Nature and Composition.* The nature of interplay between asphaltenes and metal oxides is also dependent on the orientation of functional groups present in asphaltenes, the presence of the nanoaggregates, and the properties of the adsorbent surfaces.[89] The type and composition of asphaltenes played important roles in the adsorption as the presence of carboxylic, pyridinic, thiophenic, pyrrolic, and sulfite functional groups was shown to be responsible for the favorable interaction with the metal oxide NPs.[90] Taborda et al. evaluated the C7 asphaltene adsorption onto alumina, silica, and acidic silica NPs by an UV−vis spectrophotometry method[77] and found that the asphaltene adsorption followed in the order of $SiO_2$-acidic > $SiO_2$ > $Al_2O_3$.[77] It was suggested that $Al_2O_3$ affinity for asphaltenes[91] was due to the molecular interactions initiated by aluminol and O-, N- or S-containing groups in asphaltenes. However, it was also suggested that besides exhibiting lower surface area than those of $SiO_2$ and $SiO_2$-acidic NPs, the interactions between the hydroxyl groups of asphaltenes and the silanol groups of the $SiO_2$ surfaces are greater than the affinity for $Al_2O_3$, which favored higher adsorption onto $SiO_2$ NPs.[91] Furthermore, as the NP surfaces become more acidic, the number of silanol groups is increased, enhancing more efficient asphaltene adsorption onto $SiO_2$-acidic surfaces.[78]

Moreover, asphaltene self-association also played a significant role for asphaltene adsorption onto different metal oxides. To estimate the effect of asphaltene self-association on adsorption, Guzmán et al. evaluated two methods for determining experimental adsorption isotherms for asphaltenes extracted from heavy oils onto three different types of NPs (fumed $SiO_2$, magnetite, and $SiO_2$ NPs).[72] The authors performed batch adsorption tests: (i) exposing a certain mass of NPs (5, 10, 20 g/L) in a fixed volume of toluene while changing the initial asphaltene concentration (100−2000 mg/L) and (ii) exposing a given asphaltene amount (500, 1000, 1500 mg/L) in a fixed solvent volume (Heptol, 60/40 ratio of *n*-heptane/toluene) while varying the dosage of NPs (1−25 g/L). The results showed that for both methods the asphaltene adsorption was higher from the Heptol system due to an increase in asphaltene self-association compared to the toluene system, and the greatest adsorption affinity was achieved for magnetite NPs, followed by fumed $SiO_2$, and $SiO_2$ NPs. The difference in the adsorbed amounts for fumed $SiO_2$ and $SiO_2$ NPs could be explained by the differences in surface acidities and disposition of silanol groups onto the NPs. Moreover, the shape of the adsorption isotherm was more dependent on the used method, which was attributed to the self-associative behavior of asphaltenes. It was shown that both methods lead to results with different implications. However, the authors suggested that the second method is more precise for determination of the optimal amount of NPs in the liquids used for different asphaltene related problems.[72] Similar results were reported when adsorption of asphaltenes onto $SiO_2$ NPs were increased as follows: Heptol 50 > Heptol 20 > toluene.[86] In other paper, Nassar showed that adsorption of asphaltenes onto $\gamma$-$Al_2O_3$ NPs was dependent on the initial asphaltene and heptane/toluene ratio (H/T). Adsorption was increased by following the increase in initial asphaltene concentration and H/T, which was attributed to greater asphaltene self-association.[68]

*2.1.5. Solvents Used for Extraction of Asphaltenes.* Asphaltenes can be separated from crude oils by using nonpolar solvents (paraffinic, e.g., *n*-pentane and *n*-heptane), forming precipitate that can be filtered and may dissolve in aromatic compounds for further use. The asphaltenes separated by *n*-pentane and *n*-heptane are named as C5-asphaltene and C7-asphaltene, respectively. It was found that the $Q_{max}$ of C7-asphaltenes was slightly higher than that of C5-asphaltenes adsorbed onto metal oxide surfaces. This can be explained by the higher polarity and aromaticity of the C7-asphaltenes compared to C5-asphaltenes; i.e., C7-asphaltenes contained lower amounts of resins than C5-asphaltenes, and this would influence their colloidal behavior also impacting the interactive forces between the asphaltenes and NPs.[74] Furthermore, it was also shown that the adsorption of n-C7-asphaltenes increased greatly at low equilibrium concentration and started to level off, suggesting that the NPs have high adsorption affinity for n-C7-asphaltenes even at low concentrations.[89]

*2.1.6. Molecular Weight of Asphaltenes.* The adsorption rate, affinity, and capacity were also found to be dependent on the MW of asphaltenes. It was found that when thermally cracked asphaltenes were adsorbed onto $Fe_3O_4$ NPs, the adsorption capacities were greatest for the lower MW asphaltene molecules. At the same time, the adsorption affinity


https://doi.org/10.1021/acs.energyfuels.1c01990
Energy Fuels 2021, 35, 19191−19210

was strongest for the molecules with largest MW.[73] Later, Vargas et al. used surface-modified $SiO_2$ NPs to study the asphaltene adsorption from toluene solution.[71] They found that the surface-modified NPs showed adsorption enhancement in the order of $SiO_2$-cellulose > $SiO_2$-chitosan > $SiO_2$-polyethylene glycol > $SiO_2$. The images from scanning electron microscopy (SEM) and size distribution intensity from the dynamic light scattering (DLS) suggested that the polar active groups exposed in the functionalized NPs showed a preferential interaction with the low MW molecules present in asphaltenes.[71]

*2.1.7. pH Effect.* The interactions between NPs and asphaltenes can be changed at different pH conditions. In one of the studies, Fourier-transform infrared spectroscopy (FTIR) was performed at different pH conditions on the precipitated phase to investigate the interactions between $TiO_2$ nanofluids and asphaltenes. For this purpose, the onset of asphaltene precipitation was determined by *n*-heptane titration of oil samples in the presence of $TiO_2$ nanofluids. The results revealed that at acidic conditions, $TiO_2$ nanofluids in the crude oil phase may cause changes in the *n*-heptane insoluble asphaltenes structures and made the asphaltene network more stable by formation of the hydrogen bonds (H-bonds) between asphaltene nanoaggregates and the NPs. At basic conditions, the strength of the H-bonding could be reduced and less molecular attachment would be happening.[92]

*2.1.8. Effect of Water.* Water is present at multiple stages during crude oil recovery, upgrading, and processing. It was revealed that asphaltene adsorption decreased onto $\gamma$-$Al_2O_3$ NPs from a toluene solution at increased water content. Water enhanced the water affinity of the NP surfaces, pushing the asphaltenes further away from the potential adsorption sites. Water also contributed to NP aggregation impacting their adsorption capacity.[68] It was suggested that in the presence of water, asphaltenes act as surface-active substances leading to emulsion formation and stabilization. This would decrease the adsorption, as the asphaltenes attract more toward water droplets rather than the NPs.[93] However, in one of the studies, where synthesized $Fe_2O_3$ was used, the addition of water did not have a major impact on asphaltene adsorption.[88]

*2.1.9. Effect of Temperature.* Heat treatment in the presence of metal oxide NPs reduced asphaltene adsorption due to NP agglomeration and corresponding reduction of the available surface area.[88] Furthermore, elevating the temperature also caused a reduction in asphaltene self-association,[68] changing the spatial disposition over the surface of adsorbent and weakening the intermolecular forces between the adsorbate and adsorbent.[68,94] It was observed that the asphaltene adsorption was decreased by 20% as the temperature increased when n-C7 asphaltenes were adsorbed onto silica NPs from solvent (toluene + heptane).[86] Similar results were found when asphaltenes were adsorbed onto $\gamma$-$Al_2O_3$ NPs from a toluene solution.[68]

*2.1.10. Effect of Pressure.* Asphaltene adsorption onto $SiO_2$ NPs increased with pressure[86] as the intermolecular interactions (e.g., H-bonds, induction, dispersion, and electrostatic forces) between adsorbate−adsorbate became stronger. This may also cause increased affinity between asphaltenes and metal oxide surfaces.[94]

**2.2. Hybrid NPs.** Several authors studied the asphaltene adsorption by various contents of NiO NPs supported on different nanoparticulated matrices. It is observed that the initial asphaltene concentration did not have an effect on asphaltene adsorption onto hybrid NPs, which adsorbed more asphaltenes than the support materials. The nanosized dimensions and high dispersibility of the NPs lead to suitable interactions with asphaltenes.[95−98] In another study, asphaltene adsorption by a hybrid nanomaterial made of NiO NPs (15 nm) supported on a silica gel nanoparticulated matrix (90 nm) was analyzed. It was reported that at constant temperature (25 °C) asphaltene adsorption onto the hybrid nanomaterials grew with increasing NiO content. However, by increasing the temperature, the asphaltene adsorption was slightly decreased.[95] In another study, different types of hybrid nanomaterials (e.g., SNi15, a nanohybrid material synthesized using nanosilica gel support containing 15 wt % $Ni(NO_3)_2$) were used to evaluate asphaltene adsorption efficiency.[96] It was observed that asphaltene adsorption from the toluene solution reduced as follows: AlNi15 > SNi15 > SNi5 > AlNi5 ≈ silica gel (amorphous) > silica gel (crystalline) > AlII > fumed silica gel > zeolite > PdNi/Al > Al > washed rock ≈ unwashed rock > silica gel (commercial). Furthermore, the adsorption equilibrium onto all hybrid nanomaterials was rapidly achieved within 2 min.[96] Later, Franco et al. also analyzed the effects of NiO content (AlNi5 = 5% Ni $(NO_3)_2$ and AlNi15 = 15% $Ni(NO_3)_2$) on the asphaltene adsorption onto hybrid nanomaterials made of NiO NPs supported on a $Al_2O_3$ matrix.[97] Their results revealed that the adsorption of asphaltenes onto NiO supported on $Al_2O_3$ (125.7 mg/g) was much higher than that over $Al_2O_3$ (63.4 mg/g) alone. Moreover, the asphaltene adsorption followed the order of AlNi15 > AlNi5 > $Al_2O_3$, and complete asphaltene sorption onto NiO supported on nanoparticulated $Al_2O_3$ could be achieved in just 2 min.[97] Franco et al. functionalized fumed $SiO_2$ NPs with Ni and Pd and investigated the adsorption of asphaltenes obtained from heavy crude oil samples.[98] It was shown that adsorption onto NiO and/or PdO supported on fumed $SiO_2$ was much more efficient than that onto the unmodified fumed $SiO_2$. The authors further revealed that for all the NP samples, the adsorption equilibrium was reached within the first 10 min of the experiment in the following order: SPd1 ≈ SNi0.66Pd0.66 > S ≈ SNi1 ≈ SNi2 > SPd2 ≈ SNi1Pd1. It was concluded that SNi1Pd1 and SPd2 NPs had faster adsorption kinetics and greater asphaltene uptake than other NPs.[98] The high rate of asphaltene adsorption by NiO NPs was attributed to the intermolecular forces (i.e., electrical forces and polar interactions) between the polar functional groups and heteroatoms in asphaltene structure and the NiO supported on various nanoparticulated matrices. Furthermore, the high affinity toward asphaltenes was attributed to the good dispersion of NiO on the surfaces of the support matrix.[95,96,98]

NiO-based hybrid NPs, $Fe_3O_4$ NPs supported by chitosan ($Fe_3O_4$@CHI), and silica NPs ($Fe_3O_4$@$SiO_2$) were tested for asphaltene adsorption from toluene solutions.[99] The results revealed that the $Fe_3O_4$@CHI NPs adsorbed significantly higher amounts of asphaltenes, and the amounts of asphaltenes adsorbed onto different NP surfaces were as follows: $Fe_3O_4$@chitosan > $Fe_3O_4$ > $Fe_3O_4$@$SiO_2$ > $SiO_2$ > chitosan. Furthermore, it was noticed that the adsorption differences increased at a higher concentration range of the NPs and had a direct relationship to the concentration of asphaltenes. The authors proposed that the high adsorption of asphaltenes onto $Fe_3O_4$ is due to the molecular interactions between $\pi$ electrons in aromatic rings with Fe in $Fe_3O_4$ NPs.[99]

**2.3. Carbonaceous Nanostructures.** The adsorption of heavy crude oil asphaltenes from a solution of 37 vol % of


https://doi.org/10.1021/acs.energyfuels.1c01990
Energy Fuels 2021, 35, 19191−19210

Table 2. Summary of Crude Oil Demulsification by Nanoparticles (NPs)

| Types of NPs | Experimental Conditions | Removal efficiency | Eq. time | Recycling tests | ref |
|---|---|---|---|---|---|
| **$Fe_3O_4$NPs** | | | | | |
| $Fe_3O_4$ | Water in bitumen (5 wt % water) emulsion at 80 °C | 16% | 1 h | 10 cycles | 103 |
| $Fe_3O_4$-$SiO_2$ | NPs addition 1.5 wt %; 0.15 g/10 g emulsion; external magnetic field | 34% | | | |
| $Fe_3O_4$-$SiO_2$-$NH_2$ | | 22% | | | |
| $Fe_3O_4$-EC (M-EC) | | 94% | | | |
| EC | | 90% | | | |
| $Fe_3O_4$-EC (M-EC) | Water in toluene (1:4 W/W) emulsion; 0.2 wt % asphaltenes | 100% | 10 s | | 104 |
| | NPs addition 1 wt %; 0.05 g/5 g emulsion; external magnetic field | | | | |
| $Fe_3O_4$-EC-CMC (M-Janus) NPs | Water in bitumen (5 wt % water) emulsion at 25 °C; NPs addition 1 wt % (0.1 g/10 g emulsion); external magnetic field | 95% | 30 min | 5 cycles | 105 |
| $Fe_3O_4$@OA | Cyclohexane-diluted crude oil-in-water (cyclohexane-diluted crude oil, Tween 60, deionized water) emulsions at 25 °C; NPs addition 1−10 wt % (0.1−1 g/10 mL emulsion; external magnetic field | 0−97% | 12 h | 5 cycles | 106 |
| $Fe_3O_4$ | | 0−50% | | | |
| $Fe_3O_4$-CMC-EC | Water in naphtha diluted bitumen (5 wt % water) emulsion at 25 °C | 90% | 24 h | several | 108 |
| | NPs addition 100 mg/10 g emulsions; external magnetic field | | | | |
| $Fe_3O_4$-$SiO_2$-KH-1231 | Water in oil (1 mL water, 100 mL model oil, 0.5 g span 80) emulsions at 25 C; NPs addition 0.4 g/10 mL emulsion | 90% | 2 h | 6 cycles | 109 |
| $Fe_3O_4$-P (MMA-AA-DVB) | Heavy crude oil-in-water (30%−50% water) emulsions at 60 °C; NPs addition 500 ppm in 10 mL emulsions; external magnetic field | 95% | 2 h | 5 cycles | 60 |
| $Fe_3O_4$-Basorol P DB-9935 (M-DB) | Light crude oil-in-water emulsions, optimum dosage 0.98 ppm at 38.2 °C | 95% | 1 h | | 111 |
| | Medium crude oil-in-water emulsions, optimum dosage 0.99 ppm at 45.2 °C | 88% | | | |
| | Heavy crude oil-in-water emulsions, optimum dosage 1.1 ppm at 50.1 °C | 82% | | | |
| EP@APTES-Fe3$O_4$ | Oil-in-water (2 g oil in 198 g water) emulsions at 25 °C; NPs addition 100−600 mg/L | 95% | 10 min | 4 cycles | 112 |
| $Fe_3O_4$-PDMAEMA | Oil-in-water (2.5 wt % diesel oil in water) emulsions at 25 °C; NPs addition 0.4 g/mL; external magnetic field | 90% | 1 min | 6 cycles | 66 |
| **GO-Nanosheets** | | | | | |
| GO-Nanosheets | Oil-in-water (1−100 g crude oil/L water) emulsions at 25 °C, optimum dosage of nanosheets 30 mg/L | 99.9% | 2 min | | 119 |
| GO-Nanosheets | Oil-in-water (20 g crude oil/380 g water) emulsions at 25 °C; optimum dosage of nanosheets 40 mg/L | 99.87% | 30 min | | 121 |
| rGO-110 Nanosheets | | 99.97% | | | |
| GO-A Nanosheets | Oil-in-water (1 g crude oil/L water) emulsions at 25 °C; dosage of nanosheets 100 mg/L | 96.8% | 15 min | | 122 |
| M-GO nanosheets | Oil-in-water (5 wt % oil concentration) emulsions at 25 °C; optimum dosage of nanosheets 0.25 wt % | 99.98% | 5 min | 6−7 cycles | 123 |
| GO-$SiO_2$ | Water in crude oil (2:3 v/v) emulsions at 25 °C | 100% | 90 min | | 124 |
| $SiO_2$ NPs | Optimum dosage of $SiO_2$ 500 ppm | 100% | 110 min | | |
| $SiO_2$-OA | Optimum dosage of GO-$SiO_2$ and $SiO_2$-OA 300 ppm | 37.5% | | | |
| $SiO_2$-SDBS | Optimum dosage of $SiO_2$-SBDS 500 ppm | 84% | | | |
| **$SiO_2$-NPs** | | | | | |
| $SiO_2$-Hydrophobic | Water-in-cyclohexane emulsions (69.96 wt % cyclohexane, 29.96 wt % water, 0.08 wt % Span 80), NPs dosage 0.1−1.3 wt % | 0% postmix | 5 min | | 125 |
| | | 5% premix | | | |
| $SiO_2$-Hydrophilic | | 10% postmix | | | |
| | | 55% premix | | | |
| $SiO_2$-Partially hydrophobic | | 88% postmix | | | |
| | | 0% premix | | | |
| $SiO_2$ | Water in oil (5 wt % water) emulsions at 65 °C | 60% | 24 h | | 141 |
| $SiO_2$-PVA | | 90% | | | |
| **$TiO_2$-NPs** | | | | | |
| $TiO_2$ | Water in oil (5 wt % water) emulsions at 60 °C; NPs dosage 0.03 wt % | 90% | 4 h | | 59 |
| | Water in oil (80 mL water/200 mL crude oil) emulsions; optimum NP dosage 500 mg/L at 75 °C | 93.5% | 3 h | | 132 |
| **M-MWCNTs** | Oil-in-water (1 wt % oil) emulsions, optimum NP dosage 400 mg/L at room temperature, pH 6 | 95.55% | | 5 cycles | 133 |
| **CNTs/$SiO_2$** | Oil-in-water (500 mL water/142 mL oil) emulsions, optimum NP dosage 500 mg/L at 70 °C | 87.4% | 30 min | | 134 |

Heptol onto a number of carbonaceous nanostructures (reduced graphene oxide (rGO), multiwalled carbon nanotubes (MWCNTs), carbon black (CB), and activated carbon (AC)) were investigated by Mansoori Mosleh et al.[70] Among



https://doi.org/10.1021/acs.energyfuels.1c01990
Energy Fuels 2021, 35, 19191−19210

other adsorbents, the rGO exhibited the greatest asphaltene adsorption capacity (640 mg/g), which was 5.7, 2.4, and 1.2 times higher than those of the AC, CB, and MWCNTs samples, respectively. The reported asphaltene adsorption capacity decreased in the following order: rGO > MWCNTs > CB > AC, and the rGO sample was 6.6 and 2.6 times more effective than those of AC and CB, respectively. Furthermore, equilibrium adsorption was achieved after 1, 4, 12, and 24 h for rGO, MWCNTs, CB, and AC, respectively. The interactions of the asphaltenes with the surface sites on the investigated adsorbents were indicated to be nearly irreversible and resulted from a combination of van der Waals, polar, electrostatic, and $\pi-\pi$ interactions. It was reported that the addition of water to the heptane in the toluene solution had no effect on the asphaltene adsorption capacity. The capacity had, however, increased proportionally to the increased heptane fraction in Heptol solutions.[70]

**2.4. Coated NPs.** Polythiophene (PT) exhibits special structural properties and is widely investigated as a coating material for various magnetic NPs. It was found by Skartlien et al. that polymerized PT contains several sulfur heterocycles.[100] The polarity of PT is high, which increases its ability to interact with the heteroatoms in asphaltene molecular structures. Setoodeh et al. applied a PT coating onto magnetic $Fe_3O_4$ NPs and investigated asphaltene adsorption from a toluene solution and crude oil mixture.[101] The results indicated that the $Fe_3O_4$-PT magnetic NPs had higher asphaltene adsorption than the uncoated $Fe_3O_4$ samples, and equilibrium was established during the first 2 h. As a result of the high polar interactions between the PT and asphaltenes, the coated NPs removed more asphaltenes. The authors registered that the $Q_{max}$ values for the $Fe_3O_4$ and $Fe_3O_4$-PT samples were 0.79 and 1.09 mg $m^{-2}$, respectively, with the optimum value of NP concentration at about 10 g/L. Moreover, increased temperatures lead to less efficient asphaltene adsorption, and higher pressures lead to the opposite. The asphaltene adsorption onto NPs increased with decreasing NP concentration, and more efficient adsorption was registered when the initial asphaltene concentration was increased. The authors found that the $Fe_3O_4$-PT NPs were able to adsorb asphaltenes directly from crude oil in a similar manner as in the case of a synthetic asphaltene−toluene solution.[101] Setoodeh et al. also evaluated performance of the $Fe_3O_4$ NPs coated with PT, Mil-101 (Cr) (MOF), graphene oxide (GO), $SiO_2$, and chitosan for asphaltene adsorption from crude oil in a continuous and bench scale setup, while keeping the NPs concentration at 10 g/L.[102] They found that the PT coating had the highest capacity for adsorption of asphaltenes, and the asphaltene adsorption capacity of the substrates decreased in the following order: PT-$Fe_3O_4$ > MOF-$Fe_3O_4$ > GO-$Fe_3O_4$ > chitosan-$Fe_3O_4$ > uncoated $Fe_3O_4$ > $SiO_2$-$Fe_3O_4$. Furthermore, it was revealed that the adsorption efficiency grew with the contact time. The equilibrium was attained after 2 h in both test cases, which is also in agreement with the previous study.[102] Moreover, it was observed that the quantity of adsorbed asphaltenes was lower in continuous tests than in the batch tests.[102]

## 3. CRUDE OIL DEMULSIFICATION USING NANOPARTICLES

In this section, crude oil demulsification using various types of NPs studied by different authors is discussed and summarized in Table 2. NPs with high surface areas adsorb asphaltenes efficiently, which also leads to the weakening of the rigid interfacial films between emulsion droplets. Moreover, interfacially active magnetic NPs also adsorb at the droplet surfaces and contribute to higher coalescence rates under magnetic field. Consequently, both mechanisms resulted in more efficient demulsification of crude oil−water emulsions. The rate of separation depends on many parameters, and these parameters are discussed in the following section.

**3.1. Demulsification of Crude Oil Emulsions by Magnetic NPs.** Magnetic NPs functionalized with various interfacially active groups were used in several investigations for demulsification of crude oil emulsions.[60,66,103−112] These magnetic NPs were also responsive to external magnetic force and can assist in removing water from emulsions. In research by Peng et al., ethyl-cellulose-grafted $Fe_3O_4$ (M-EC) NPs were prepared and tested for water separation from a naphtha-diluted bitumen emulsion. Later on, these NPs were removed by a magnetic field at 80 °C.[103] After addition of 1.5 wt % M-EC, more than 90% of water was removed from the diluted bitumen emulsion. The process was 10 times faster than demulsification by ethyl cellulose itself. The chemically bounded EC on the surface of magnetic NPs leads to the high demulsification efficiency. Moreover, the authors confirmed that the regenerated M-EC was chemically stable and retained its interfacial activity as it was effective in demulsification of diluted bitumen emulsions even after 10 cycles. Here, 80% of water was removed from industrial bitumen froth after adding M-EC and applying an external magnetic field for 2 min at room temperature.[103] In a follow-up study, interfacially active M-EC NPs were also used for separation of W/O (water/toluene; 1/4, w/w) emulsions stabilized by 0.2 wt % of asphaltenes.[104] The demulsification was achieved by adding 0.05 g of M-EC into 5 g of emulsion at room temperature. The magnetic M-EC NPs accumulated at the interfaces and attached to the water droplets. It was observed that when a magnetic field was applied, the M-EC NPs enhanced the coalescence of droplets by rapid migration in the direction of the magnet. Due to the application of an external magnetic field, a rapid phase separation occurred in less than 10 s.[104]

Later, for dewatering of W/O emulsions in the heavy oil industry and removal of oil from the O/W emulsion created during oil spills, He et al. designed and synthesized novel magnetically responsive and interfacially active Janus (M-Janus) NPs with hydrophobic ethyl cellulose (EC) and hydrophilic carboxymethyl cellulose (CMC) coatings on the opposing sides of the $Fe_3O_4$ NPs.[105] The results revealed that the M-Janus NPs had high efficiency in separating both water from W/O emulsion and oil from oily waste waters. The M-Janus NPs were highly interfacially active with 95% separation efficiency even after five cycles.[105] It was suggested that due to the steric repulsion and electrostatic forces created by the coated celluloses on the NP surfaces, M-Janus NPs had excellent dispersion in either organic or aqueous phases and exhibited excellent performance in phase separation of both the oily wastewaters and the water-in-diluted bitumen emulsions.[105]

Liang and co-workers produced single-layer oleic acid-coated $Fe_3O_4$ ($Fe_3O_4$@OA) NPs and studied their efficiency for destabilization of cyclohexane-diluted crude oil-in-water emulsions under an external magnetic field.[106] It was demonstrated that the $Fe_3O_4$@OA NPs can demulsify O/W emulsions, and the demulsification efficiency ($E_D$) was affected


https://doi.org/10.1021/acs.energyfuels.1c01990
Energy Fuels 2021, 35, 19191−19210

by the concentration and wettability of the NPs as well as operational parameters. They observed that by increasing the $Fe_3O_4$@OA dosage and at certain wettability (water contact angle, $\Theta_w \sim 90°$), $E_D$ of ~97% was achieved.[106] It was previously revealed by Lan et al. that $Fe_3O_4$@OA NPs with $\Theta_w \sim 90°$ strongly accumulated at interfaces, which enhanced the droplet coalescence rate and imparted their magnetic properties in the oil phase. These magnetically active droplets could be efficiently separated from the water phase by applying an appropriate magnetic field.[107] Furthermore, demulsification efficiency was almost constant in the pH range of 4.0−7.5 but gradually decreased as the pH was increased from 8.0 to 11.0. It is mentioned that the $Fe_3O_4$@OA NPs had good recyclability, and the demulsification efficiency of the recycled $Fe_3O_4$@OA did not change significantly even after five cycles of demulsification.[106] In another study, Liang et al. prepared magnetically responsive composite NPs comprising the outer layer of interfacially active materials and an inner magnetic core. To prepare these NPs, first, $Fe_3O_4$ NPs were primed with CMC, and then, EC was adsorbed onto the CMC-primed NPs.[108] The authors reported that a quick demulsification of naphtha-diluted bitumen emulsions was achieved by applying their composite NPs. The results showed that more than 90% dewatering efficiency was achieved after 24 h when $Fe_3O_4$-CMC-EC NPs were used, and an external magnetic field was applied on naphtha-diluted bitumen emulsions. The NPs were recovered by a treatment in a mixture of toluene and alcohol, and the recovered particles were reused in several repetitive applications. On the basis of the results, the authors suggested that the interfacially active magnetic NPs have a great potential in treating multiphase wastes from industrial processes, separation vessels, and storage tanks. The NPs can be separated by a magnetic field without the need for shutdowns or interruption of the processes.[108]

Chen et al. prepared $Fe_3O_4$ NPs by coating amorphous $SiO_2$ and further functionalization with a dodecyltrimethoxysilane (KH-1231).[109] It was demonstrated that the surfactant-stabilized W/O emulsions were destabilized rapidly, and the quantity of NPs strongly influenced the separation rate and efficiency. The NPs were removed by the magnetic field, and after a recovery treatment, could be used for six cycles while maintaining high efficiency and durable magnetic response. Authors suggested that the NPs were effective for treatment of various oils and solvents (e.g., *n*-hexane, toluene, gasoline, *n*-octane, *n*-decane), and applicable for the treatment of large-scale emulsion volumes.[109]

Ali and coworkers designed interfacially active and magnetically responsive poly(methylmethacrylate-acrylicacid-divinylbenzene) (P(MMA-AA-DVB)/$Fe_3O_4$ magnetic composite NPs with raspberry-like structures. They observed that P(MMA-AA-DVB)/$Fe_3O_4$ NPs demonstrated effective demulsification efficiency for originally stable W/O emulsions at 60 °C after 1 h.[60,110] Furthermore, it was shown that the emulsion breaking started after 10 min and was enhanced with an increase in temperature. The maximum effect was reached after 60 min and resulted in full separation of the water phase. It was suggested that the increase in temperature resulted in reduced viscosity of the W/O emulsion and led to easing of the adsorption of P(MMA-AA-DVB)/$Fe_3O_4$ NPs at the oil−water interface. It was proposed that the carboxylic groups made the NPs more interfacially active, which consequently enhanced droplet coalescence and their rapid separation from the oil phase. Later, NPs were recovered by washing with a solvent, and the recycled particles showed no alterations in the separation efficiency after five cycles.[60]

The effect of $Fe_3O_4$-Basorol P DB-9935 (M-DB) NPs on demulsification efficiency of light, medium, and heavy crude oils was investigated by Farrokhi et al. at different operating temperatures.[111] It was observed that there was a limit range of NP concentration for dewatering of each W/O emulsion based on its viscosity. The optimum concentrations of M-DB were achieved at 1.1. 0.99, and 0.98 ppm, while the optimum temperatures were suggested to be 50.1, 45.2, and 38.2 °C for light, medium, and heavy crude oils, respectively. Furthermore, the results showed that by increasing temperature and NP concentration, the dewatering efficiency will improve (on a reasonable range based on the viscosity of crude oils). The temperature effect was more prominent on the dewatering efficiency than the NP concentration. The application of the magnetic field increased the dewatering efficiency by 5%−20% and decreased the droplet settling time.[111]

Xu et al. modified the expanded perlite (EP) by 3-aminopropyl triethoxysilane (APTES) to form the EP@APTES and then grafted $Fe_3O_4$ NPs onto the surface of EP@APTES to synthesize the EP@APTES-$Fe_3O_4$ composite. EP@APTES-$Fe_3O_4$ was used for treating oil-in-water (1 wt % oil) emulsions, and the effects of pH, NP loading, and salt concentrations in water phase were evaluated. The results revealed that EP@APTES-$Fe_3O_4$ exhibited excellent salt resistance and demulsification efficiency at pH of 6.0, 4.0, and 2.0. Furthermore, EP@APTES-$Fe_3O_4$ could be recycled for up to four cycles with minor loss in the demulsification efficiency. Under the neutral and acidic conditions, EP@APTES-$Fe_3O_4$ NPs were charged positively, and onto these NPs surfaces, oil droplets could be effectively coupled via electrostatic attraction, which subsequently enhanced oil−water separation.[112]

Core−shell hybrid magnetic NPs were designed by Wang et al. for separation of emulsified oil from water.[66] The synthesized hybrid NPs contained a magnetic $Fe_3O_4$ NP cluster as the core and poly(2-(dimethylamino)ethyl methacrylate) (PDMAEMA) as arms, showing dual stimuli responsiveness to both magnetic field and pH. They reported that the polymer arms were sensitive to pH, which could alter the NPs surface polarity to reversibly form and destabilize O/W emulsions. The separation of 2.5 wt % emulsified diesel oil from water was completed in four different steps. In the first step, NPs were added to the emulsion under a specific pH. Afterward, a magnetic field was applied, which concentrated the NP-coated oil droplets from water, and 90 wt % of water recovery was achieved by decantation. During the third step, the pH of water was decreased in the diesel-in-water emulsion, which consequently destabilized droplets and led to phase separation. In the fourth step, the NPs were recovered and reused for subsequent oil separation from water. It was further reported that the NPs could be recycled for up to six times without losing their functionality and efficiency.[66]

**3.2. Demulsification of Crude Oil Emulsions Using Graphene Oxide Nanosheets.** Graphene has attracted enormous interest due to its low cost, availability, and broad functionalization possibilities.[113] A two-dimensional (2D) honeycomb lattice-type structure like graphene oxide (GO) consists of a flat carbon monolayer arranged in a hexagonal lattice structure. Besides, it has a basic layer of graphitic building blocks.[113] GO also generated high interest due to its robust characteristics. It is a hybrid material with high


https://doi.org/10.1021/acs.energyfuels.1c01990
Energy Fuels 2021, 35, 19191−19210

adsorption capacity. GO is also shown to be more selective toward heavy thiophenic hydrocarbons. The addition of GO increases adsorption of theophenic organosulfur compounds present in crude oils by 170%. The ultrafine pores of GO can filter separated adsorbent particles by generating active sites. Thus, they are referred to as a relatively better sorbent than Ni in removal of sulfur compounds. At the same time, GO does not represent as strong catalytic characteristics as Ni.[114,115] Hydroxyl, carboxyl, and epoxy groups are added by graphite oxidation enabling GO to become an efficient surfactant with a hydrophobic basal plane and hydrophilic surface groups.[116,117] This attribute allows GO to be used as a surfactant for stabilization of water/air and water/oil interfaces.[118] GO is also suggested as an excellent substrate for oil and water demulsification applications.

GO nanosheets were used by Liu et al. as a demulsifier of O/W emulsions with 99.9% of oil being separated within a few minutes (at ∼30 mg/L).[119] It was observed that the GO was not only useful for ordinary crude oil emulsion separation but also to break extra heavy oil emulsions. However, the results also indicated that demulsification was influenced by the crude oil properties, its content in an emulsion, GO loading, and pH. It was revealed that preferential distribution of the GO either in oil or water phases after emulsion separation was pH dependent. The authors attributed the prominent demulsification ability of GO to the strong interactions between the GO and asphaltene/resin molecules. Figure 5 illustrates the GO

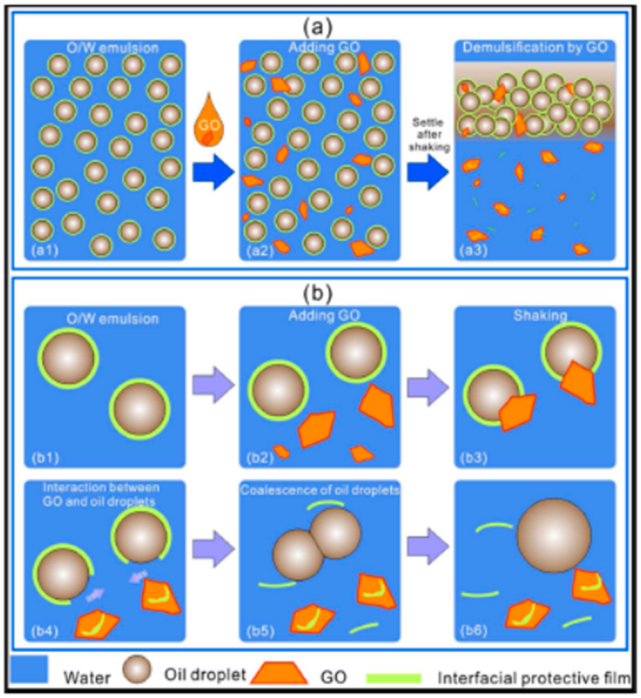


**Figure 5.** Schematic illustration of demulsification processes (a) and possible mechanism for coagulation of oil droplets driven by GO nanosheets (b).[119]

nanosheet-driven mechanism for the oil droplets coagulation leading to demulsification. Once the GO nanosheets were added into the O/W emulsion, the nanosheets uniformly dispersed in the water phase and reached the interfaces to contact the surface-active molecules (Figure 5a2, b2). Due to the strong GO and asphaltenes interaction (Figure 5b3), the protective film got partially destroyed. This destruction causes a noncontinuous interfacial film due to collisions (Figure 5b4). The film destruction generates coalescence sites for smaller oil droplets to grow (Figure 5b5). The coalescence and aggregation of the droplets (Figure 5b6) leads to continuous oil phase formation and upward movement (Figure 5a3). Finally, the oil is successfully separated from water.[119] Fang et al. also studied the demulsification of O/W emulsions using GO nanosheets.[120] This was found to be dependent on the interfacial GO activity and diffusion at the O/W interface. It was reported that, after addition of the GO, the emulsion stability was disrupted, and oil/water separation process had increased further with increasing temperature and GO dosage.[120] Wang et al. investigated the demulsification performance of the reduced graphene oxide (rGO) nanosheets by increasing the degree of GO reduction. The effects of the crude oil type, pH, and salinity of the water phase were studied.[121] It was found that under hydrothermal reduction of GO the $\pi$-conjugated aromatic network area on the basal plane of the GO sheets had increased, which increased the adsorption capacity and amphiphilicity of the rGO. The GO nanosheets demulsification performance improved and was enhanced with increasing reduction degree of the GO. This could be due to higher material hydrophobicity caused by a decrease in the surface polarity of the GO sheets. More than 99.9% of crude oil was recovered from the emulsion by gravity settling at ambient temperature after 30 min. The authors suggested that the increase in the absorption capacity enables a $\pi-\pi$ interaction between the rGO and the asphaltenes leading to easier disruption of the interfacial film. This eventually promoted oil droplets to coalesce and enhanced separation of oil from water. Furthermore, it was revealed that for both GO and rGO the demulsification efficiency declined in the alkaline solution due to the deprotonation of carboxyl and hydroxyl groups. This increased the electrostatic repulsion between the GO nanosheets and oil phase. It was suggested that the salinity had some adverse influence on the demulsification performance due to the change in the interfacial properties.

Contreras Ortiz et al. tested separation of O/W emulsions using GO and amine-modified GO (GO-A) nanosheets.[122] Amphiphilic GO functionalized with amino groups was produced by Hummer's modified method. It was reported that less than 15 min was required to break up O/W emulsions, and demulsification efficiency of 96.8% was achieved with GO-A.[122] Later, Liu and coworkers synthesized magnetic GO (M-GO) for separating O/W emulsions and developed a methodology to recycle the GO nanosheets.[123] The synthesis processes of making M-GO by a covalent strategy are illustrated in Figure 6. The separation tests revealed that M-GO could separate O/W emulsions within 15 min at a dosage of 0.25 wt % and be recycled 6−7 times without losing its demulsification ability. Furthermore, it was reported that the M-GO maintained good performance at acidic pH conditions which is attributed to the ionization of −OH and −COOH on the M-GO groups under acid conditions, which lead to the occurrence of less hydrophilic M-GO.[123]

Javadian and Sadrpoor synthesized green and cheap GO-$SiO_2$ NPs for dehydration of crude oil emulsions. It was shown that GO-$SiO_2$ had better performance compared to bare $SiO_2$ NPs, $SiO_2$@Oleic acid, and $SiO_2$@Sodium dodecyl sulfonate for demulsification of crude oil.[124] The results demonstrated that dehydration of crude oil emulsions was completed during 90 and 110 min with GO-$SiO_2$ and $SiO_2$NPs, respectively.


https://doi.org/10.1021/acs.energyfuels.1c01990
Energy Fuels 2021, 35, 19191−19210

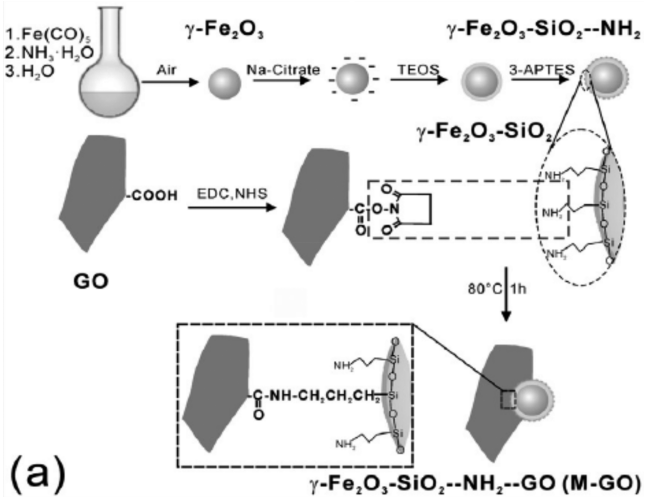


**Figure 6.** Preparation of magnetic graphene oxide.[123] Reproduced with permission from ref 123.

Better performance of the GO-$SiO_2$ NPs was attributed to the presence of aromatic rings and chains in the structure of GO that interacted with asphaltenes in the film. They could also diffuse crude oil much better and, subsequently, increase the rate of demulsification. Moreover, the functionalities (ether and carboxylic groups) present in the structure of GO caused the GO-$SiO_2$ to possess higher penetrability at the oil−water interfaces. Thus GO-$SiO_2$ reduced the IFT more effectively than $SiO_2$ NPs. Furthermore, it was demonstrated that salinity played an important role in the performance of the nanodemulsifiers. Depending on the type of the used salt, demulsification could be enhanced or diminished. The results revealed that the demulsification temperature was also an important factor. In the case of GO-$SiO_2$, dehydration time decreased from 90 to 16 min by increasing the temperature from 25 to 75 °C.[124]

**3.3. Demulsification of Oil Emulsions Using $SiO_2$ NPs.** Yegya Raman and Aichele elucidated the separation of surfactant-stabilized W/O emulsions by using $SiO_2$ NPs of different wettabilities and showed that the demulsification depends on the mode of NP addition and NP wettability.[125] Their results revealed that W/O emulsions were destabilized efficiently when partially hydrophobic NPs were added after formation of the emulsion (postmixing). The authors proposed that efficient demulsification was achieved when the surfactant depleted from the oil−water interface due to the adsorption of partially hydrophobic NPs on the surfactants which took place via H-bonding. On the other hand, it was also observed that the postmixing of hydrophobic NPs in the W/O emulsions did not result in a demulsification because of weak interactions between surfactants and hydrophobic NPs. On the contrary, the hydrophilic NPs prefer to distribute/mix in the water phase, and this preferential distribution results in a reduced adsorption of surfactants from the oil phase leading to less efficient demulsification compared to the partially hydrophobic NPs. The results showed that with $SiO_2$ NPs of different wettability, the postmixing was more efficient than premixing.[125]

Hassan et al. also used $SiO_2$ NPs in combination with a chemical demulsifier for the enhancement of crude oil demulsification process.[126] They first investigated the effect of different chemical demulsifiers (sodium dodecyl sulfate, polyethylene glycol, isopropyl alcohol, and commercial demulsifiers) on heavy crude oil emulsions and, after finding the best performing demulsifier, added $SiO_2$ NPs of two different sizes (95 and 25 nm) at concentrations of 90, 60, and 30 ppm. The results showed that the 25 nm $SiO_2$ NPs at 60 ppm concentration with a dosage of 0.5:1 for $SiO_2$ NPs to chemical demulsifier gave the best performance, and these NPs were able to remove 53% water from the emulsion.[126] Qi et al. developed interfacially active and pH-responsive $SiO_2$ NPs with poly(2-(dimethylamino)ethyl methacrylate) (DMAEMA) chains.[127] The polymer-coated $SiO_2$ NPs (DMAEMA PNPs) were tested to recover oil and afterward destabilize O/W emulsions through a variation of solution pH. The authors reported that after recovery emulsion could be destabilized by the addition of acid (pH adjustment), resulting in separation and settling of the heavy oil from the aqueous phase. Their results showed that the addition of just 0.1 wt % DMAEMA PNPs at neutral pH resulted in reduction in the water contact angle from 76° to 62°. However, after reduction of DMAEMA pH, its chains were protonated and become positively charged, and the contact angle increased from 62° to 81°. The results demonstrated the pH responsiveness of DMAEMA PNPs and their impact on the IFT, contact angle, and emulsion stability.[127] Gandomkar et al. used $SiO_2$ and $SiO_2$-PVA (poly(vinyl alcohol)) NPs for the demulsification of W/O emulsions. PVA was incorporated in the nanolayered $SiO_2$ structures with the sol−gel technique. The results demonstrated that $SiO_2$-PVA NPs increased the demulsification efficiency by about 40%.[128]

Fang Hui and Hong[129] and later Wang et al.[130] dispersed nano-$SiO_2$ particles in polyether demulsifier TA1031 and developed a new highly efficient demulsifier. Their results showed that by dispersing nano-SiO2 particles in a crude oil demulsifier at the ratio of 1:10, the time of demulsification was decreased by 30 min, and the dehydration efficiency was increased by 20%. The authors suggested that the NPs had higher interfacial activity and hydrophilicity than that of the polymer, which ruptured the oil−water interfacial film more efficiently and resulted in oil−water separation.

**3.4. Demulsification of Oil Emulsions Using $TiO_2$ NPs.** Nikkhah et al. synthesized a wide spectrum of nano-$TiO_2$ NPs by a sol−gel method with and without surfactants under different preparation conditions. The demulsification efficiencies of different NPs were analyzed by bottle and electrostatic tests.[59] The results revealed that the cetrimonium bromide (CTAB)-modified and surfactant-free $TiO_2$ demonstrated the best water separation performance and effectively increased the demulsification efficiency to greater than 90% with 0.03 wt % demulsifier optimum loading and 4 h of settling time. The electrostatic test study exhibited that in the nano-$TiO_2$ and water mixture, the dipole interactions between the water−water and water−$TiO_2$ molecules were caused by an electric field. These interactions lead to an efficient coalescence of water droplets.[59]

**3.5. Demulsification of Oil Emulsions Using Carbon Black/Nanotubes.** Wang et al. functionalized carbon black (F-CB) NPs by covalently attaching PVA onto carbon black (CB) surfaces. This was utilized in demulsification of wastewater.[131] They conducted a few bottle test studies, and the results demonstrated that a demulsification efficiency of 99.9% was achieved within a few minutes. It was suggested that the CB wettability could be altered by modifying the PVA molecules, and the improved wettability will facilitate a faster


https://doi.org/10.1021/acs.energyfuels.1c01990
Energy Fuels 2021, 35, 19191−19210

migration of particles on the oil−water interface. These F-CB NPs will interact with the natural stabilizers present in rigid interfacial film to displace them. Consequently, the coalescence of the oil droplets assisted by the F-CB NPs caused the demulsification process. The interaction mechanism between F-CB NPs and asphaltenes was investigated by the authors using quantum chemical calculations, and they found that the F-CB NPs have strong interactions with the asphaltene molecules in the form of $\Theta-\pi$ and $\pi-\pi$ forces.[131] Furthermore, Ye et al. prepared a low cost and highly interfacially active Ox-CB@$SiO_2$ by grafting nano-$SiO_2$ onto the surfaces of oxidized CB (Ox-CB) by a sol−gel method.[132] The Ox-CB@$SiO_2$ composite material was low cost with an improved demulsification performance. The authors investigated the effect of concentration of the composite demulsifier, temperature, and settling time on the demulsification of W/O emulsions by bottle tests, and 93% of water was removed with demulsifier concentration of 500 mg/L and at a temperature of 75 °C. Furthermore, the three-phase contact angle of Ox-CB@$SiO_2$ was found to be 90.2°, which confirmed that the interface is equally wetted by both phases; i.e., the demulsifier strongly accumulated at the oil−water interfaces, and the hydrophilic ends entered the aqueous phase while the hydrophobic ends entered the oil phase. Figure 7 shows the

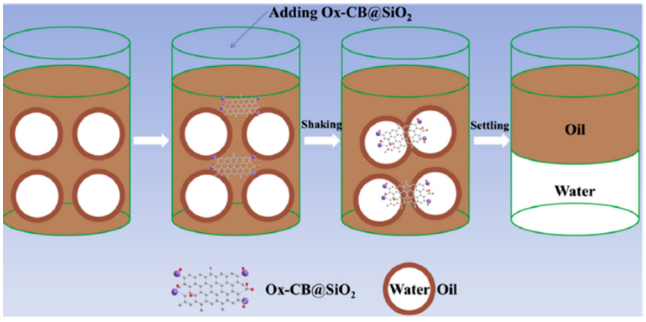


**Figure 7.** Simulation of demulsification process by interfacial-active Ox-CB@SiO2 (nano-$SiO_2$ grafted onto the surface of oxidized carbon black)[132] Reproduced with permission from ref 132.

process of simulating the demulsification. It was suggested that distribution, aggregation, and adsorption of the Ox-CB@$SiO_2$ particles at the O/W interface can effectively destroy the interfacial film, eventually, by bridging coalescence and flocculation of the droplets, enhancing the demulsification process.[132]

Carbon nanotubes are becoming attractive as a novel adsorbent due to their remarkably high adsorption capacity. Xu et al. prepared magnetically responsive multiwalled carbon nanotubes (M-MWCNTs) by introducing surface functional groups (e.g., −COOH, −OH, and $-NH_2$,) and used them for separating crude oil from O/W emulsions under acidic to alkaline conditions.[133] Furthermore, the effects of pH, salinity of the system, and the M-MWCNTs dosage on the separation efficiency were studied. The results confirmed that M-MWCNTs were as efficient demulsifiers under a wide pH range. The highest demulsification efficiency was achieved when the dosage was increased up to 400 mg/L. Furthermore, M-MWCNTs were efficiently recovered by applying a magnetic field, and these recovered particles showed good separation efficiency even after five cycles. Figure 8 depicts the demulsification mechanisms of M-MWCNTs. The authors

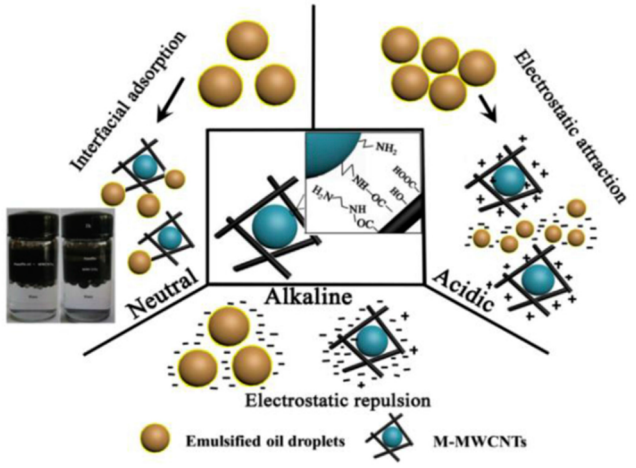


**Figure 8.** Demulsification mechanisms of M-MWCNTs under various pH levels.[133] Reproduced with permission from ref 133.

suggested that under acidic conditions separation of the crude oil from the O/W emulsion was caused by two mechanisms: (1) the electrostatic attraction between the M-MWCNTs and the asphaltenes and (2) the $\pi-\pi$ and/or $n-\pi$ interaction of aromatics/functional groups of M-WCNTs and asphaltenes. On the other hand, under neutral pH conditions, the main demulsification mechanism was the interfacial adsorption. Under alkaline conditions, due to the increase of amino groups, the electrostatic repulsion between the M-MWCNTs and O/W emulsion decreased, which consequently broke down the interfacial film and promoted oil droplet separation.[133]

Huang et al. prepared novel interfacially active and environmentally friendly carbon nanotubes (CNTs/$SiO_2$) for demulsification of water/crude oil emulsions.[134] The results demonstrated that the CNTs/$SiO_2$ nanomaterials were adsorbed effectively and rapidly onto the droplets in crude oil emulsions. A demulsification efficiency of 87.4% was reached with the optimum concentration of CNTs/$SiO_2$ nanomaterials (Figure 9). It was reported that the distribution of nanomaterials at the interfaces has improved the coalescence

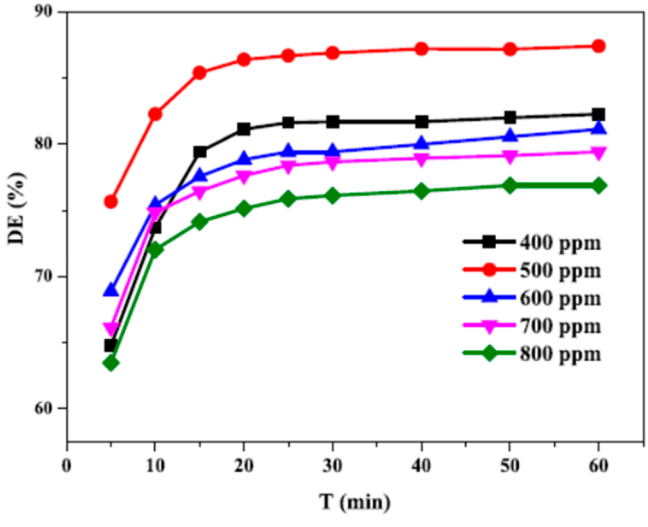


**Figure 9.** Effect of different concentrations and sedimentation times of CNTs/$SiO_2$ on demulsification efficiency.[134]


https://doi.org/10.1021/acs.energyfuels.1c01990
Energy Fuels 2021, 35, 19191−19210

of water droplets, which quickly and effectively separated water from crude oil emulsions.[134]

## 4. REMOVAL OF OIL DROPLETS FROM PRODUCED WATER BY NANOPARTICLES

Some of the authors explored the use of magnetic NPs to remove oil droplets from produced water. Pollutants like dispersed oil droplets, dissolved components, and solids must be separated from the produced water prior to its discharge or reinjection. Produced water release is a major environmental issue relating to the oil exploration industry and calls for efficient treatment processes to remove a variety of polluting components. Franco et al. investigated adsorption of oil onto hydrophobic $Al_2O_3$ and $Al_2O_3$ NPs. With an intent to reduce the oil content in oil−saltwater emulsions, these NPs were functionalized with a petroleum vacuum residue (VR) at 2 and 4 wt %. These experiments were conducted at different pH conditions (5, 7, and 9).[135] The results indicated that the maximum amount of oil was adsorbed at pH 7 using Al/4VR material. Moreover, neutral and acidic systems showed higher oil removal compared to a basic sample. Besides, increasing the amount of VR on the surface of the $Al_2O_3$ improved the removal of oil. The adsorption affinity decreased with increasing temperature, and the presence of NaCl did not affect the adsorption capacity of the NPs.[135]

Another method to remove oil droplets from water is by using magnetic NPs (Fe based) coated with a cationic surfactant developed by Ko et al.[136] It was proposed that by employing NPs with opposite surface charges, their efficient attachment to the oil droplets could be achieved. Experiments with 5 wt % decane-in-water emulsions were performed in batch-scale adsorption. Depending on the experimental conditions, decane droplets removal efficiency was in the range between 85% and 99.99%. It was suggested that electrostatic attraction between the oil droplets and cationic NPs controlled the NP attachment onto the droplet surfaces as the anionic surfactant-coated Fe NPs did not remove oil droplets. Moreover, spontaneous settling of droplets was reported when a magnetic field was applied, and the droplets settling velocity was very much dependent on the intensity of magnetic field.[136] Ko et al. also synthesized amine-functionalized Fe NPs (A-MNPs) and poly(acrylic acid) (PAA)-grafted amine-functionalized NPs (PAA-MNPs), which were used for treatment of 0.25 wt % crude O/W emulsions.[65] Positively charged A-MNPs and negatively charged oil droplets successfully attracted each other, which led to efficient oil removal in the range from 96.4% to 99.5% after 5 min of reaction between MNPs and the oil. Moreover, it was reported that the removal increase closely matched the total acid number (TAN) decrease of oil droplets. On the basis of microscopic observations, the authors suggested that the electrostatic attraction between negatively charged oil droplets and positively charged magnetic NPs controlled the attachment of NPs to the oil droplets, and the subsequent aggregation of the neutralized NPs-attached oil droplets played a critical role in efficient magnetic separation. Moreover, modeling calculations showed that the magnetic field effect on the separation velocity depended on the NP size where the smaller size contributing to faster separation.[65]

## 5. USES OF MAGNETIC NANOMATERIALS DURING OIL SPILLS

Oil spills and oil-containing wastewater discharged into open sea from ships and offshore-related applications can have severe environmental implications. Mirshahghassemi and Lead synthesized polyvinylpyrrolidone (PVP)-coated $Fe_3O_4$ NPs to separate MC252 oil from a oil-in-water mixture (oil concentration = 0.15 ± 0.05 g/L) under environmentally relevant conditions.[137] The results revealed that nearly 100% of the oil was removed from an oil−water mixture when using the PVP-coated $Fe_3O_4$ NPs. Gas chromatography and mass spectrometry analysis revealed that within 10 min close to 100% of lower MW alkanes (C9−C21) were removed by magnetic separation. Increasing the separation time up to 40 min led to removal of more than 67% of C22−25 alkanes. The NPs removed near 100% of oil from solutions made of synthetic seawater showing excellent oil removal capacity under different conditions. The authors recommended that these NPs can separate oil in a very short time duration at a great efficacy under the right environmental conditions.[137] Similar results were also reported by Palchoudhury and Lead.[138]

In other studies, conducted by Lü et al., a series of pH sensitive (3-aminopropyl)triethoxysilane (APTES)-coated $Fe_3O_4$ NPs were synthesized for their evaluation on emulsified oil from seawater separation (diesel in water emulsion, 0.2 wt % of diesel).[139] Effects of the APTES anchoring density (DA), NP dosage, and pH on oil−water demulsification were evaluated. The results revealed that under both neutral and acidic conditions, NPs with high anchoring density (DA) demonstrated enhanced separation efficiency of an oil−water system, whereas at alkaline conditions, separation was low. The authors suggested that under acidic conditions the electrostatic attraction was main driving force behind the accumulation of NPs onto oil droplet surfaces, while under neutral conditions it was mainly driven by interfacial activity (Figure 10).[139]

## 6. IMPROVEMENT OF MEMBRANE PERFORMANCE USING NANOSIZED COATINGS

For reducing membrane fouling by oil droplets, Zhou et al. modified the commercial $Al_2O_3$ microfiltration membranes by

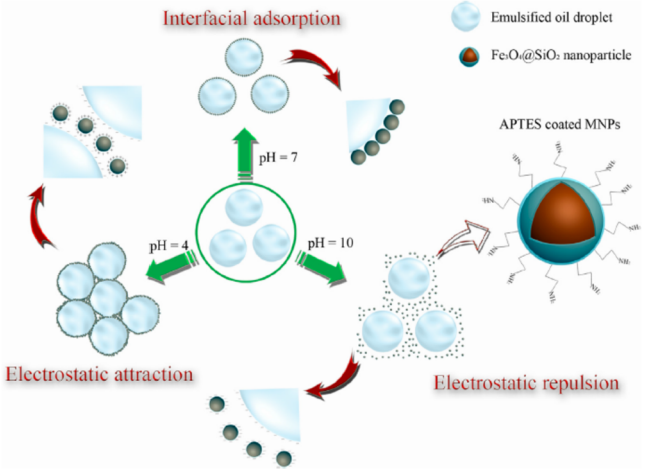


**Figure 10.** Schematic illustration of the interaction mechanism between APTES-coated MNPs and emulsified oil droplets.[139] Reproduced with permission from ref 139.


https://doi.org/10.1021/acs.energyfuels.1c01990
Energy Fuels 2021, 35, 19191−19210

the nanosized $ZrO_2$ coating.[140] The results revealed that a porous zirconia coating with a thickness of about 100 nm was formed on the membrane surface, and membrane channels made the membrane more hydrophilic. The hydrophilic nanosized coating, backflushing, and appropriate cross-flow velocity helped reduce oil fouling on the membranes. Besides, it successfully separated stable a 1 g/L engine oil−water emulsion at an oil rejection efficiency above 97.8%.[140]

## 7. CONCLUSIONS

A variety of ways of applying nanoparticles and composite nanomaterials in the oil and gas industry are explored in the current literature review. Asphaltene chemistry and crude oil composition are considered as main factors in combination with the reviewed nanomaterial properties. The focus is given to the asphaltene adsorption and emulsion separation using both magnetic and nonmagnetic nanomaterials and removal of residual oil droplets in produced water treatment, as well as minor topics where nanomaterials are used during oil spills and membrane treatments to increase antifouling resistance of separation membranes. The main conclusions are as follows:

- Certain nanomaterials exhibit higher affinity toward various asphaltene fractions than others, which is mainly attributed to their chemical structure, production and treatment methods, and surface area. A large variety of materials, production, and functionalization methods also makes it difficult to compare studies performed by different research groups. However, NiO NPs often stand out as one of the most efficient asphaltene adsorbents. Furthermore, the in situ-prepared NPs interacted better with asphaltenes, and hybrid NPs adsorbed more asphaltenes than the support materials. Overall, acid−base interaction and electrostatic attraction are found to be dominant forces for adsorption.
- Asphaltene adsorption efficiency reaches 95% for some of the studied model and crude oil systems, and asphaltene self-association played a significant role in efficient adsorption. Moreover, higher temperature led to lower adsorption, and higher pressure led to higher adsorption. Adsorption is also enhanced when the initial asphaltene concentration is increased and the NP concentration is decreased. The presence of water decreased the asphaltene adsorption onto NPs.
- Up to 100% demulsification efficiency could be achieved, while the separation time varied from 10 s to 24 h. Demulsification efficiency is affected by the properties of crude oil; oil and water contents of an emulsion; temperature, salinity, and pH of the system; concentration of NPs; and mode of NP addition. By increasing the temperature and concentration of NPs, the demulsification efficiency is increased. Also, depending on the type of used salt, demulsification can be increased or decreased. Generally, depending on the type of NPs, demulsification is improved at acidic and neutral pH as compared to basic conditions.
- Magnetic separation supported by interfacially active magnetic NPs proved to be the most powerful method for demulsification
- Up to 99.9% efficiency is reported for separation of oil droplets from produced water, and increased removal efficiency corresponded with a decrease in TAN.
- The number of recovery cycles without loss of properties varies from 1 to 7, and the recovery requires washing with solvents. Certain nanomaterials can be beneficially combined with chemical demulsifiers to improve emulsion separation.
- Surface wetting properties play an important role, as partially hydrophobic or hydrophilic NPs show promising results in emulsion separation, while hydrophobic NPs are more beneficial in produced water treatment.

## 8. KNOWLEDGE GAPS AND PERSPECTIVES

Knowledge gaps or underexplored areas identified from the current literature search are as follows:

- There is an existing lack of clear standardized criteria for evaluation of nanomaterial performance in various applications (e.g., separation of oil or water droplets, emulsion destabilization).
- Only laboratory-scale studies have so far been performed, which makes it difficult to fully evaluate potential for nanomaterial use in emulsion separation and treatment of produced water. This also explains the lack of techno-economic evaluations and life cycle analyses.
- Separation of NPs from the separated emulsion phases is rarely discussed and tested, which creates uncertainties about potential adverse environmental and health effects. However, batch experiments function well, continuous separation of NPs might become a problem. Separation of nonmagnetic NPs can also be a challenge. In the case of further crude oil processing, the presence of unseparated NPs can have some undesired effects.
- Recyclability is another important limitation as it requires use of organic solvents, and NPs can only be reused a limited number of times before losing their chemical functionality or magnetic properties.
- Asphaltene adsorption is often studied on model systems only containing asphaltene fractions. Coadsorption of other surface-active molecules (e.g., acidic components) also needs to be addressed in the studies performed on real crude oil systems.

## AUTHOR INFORMATION


### Corresponding Author

**Balram Panjwani** − *Department of Metal Production and Processing, SINTEF Industry, 7034 Trondheim, Norway;* orcid.org/0000-0002-9700-2672; Email: balram.panjwani@sintef.no

### Authors

**Umer Farooq** − *Department of Climate and Environment, SINTEF Ocean, NO-7465 Trondheim, Norway;* orcid.org/0000-0001-8310-446X

**Amit Patil** − *Department of Process Technology, SINTEF Industry, 7034 Trondheim, Norway*

**Galina Simonsen** − *Department of Process Technology, SINTEF Industry, 7034 Trondheim, Norway*

Complete contact information is available at: https://pubs.acs.org/10.1021/acs.energyfuels.1c01990


### Notes

The authors declare no competing financial interest.



https://doi.org/10.1021/acs.energyfuels.1c01990
*Energy Fuels* 2021, 35, 19191−19210

## Biographies

Dr. Umer Farooq holds a Ph.D. in chemical engineering from the Norwegian University of Science & Technology. He is currently working as a research scientist in the Department of Environment and Climate at SINTEF Ocean, Trondheim, Norway. His research interests include fundamental interfacial phenomena in the oil industry, fluid characterization, oil fate and behavior, dispersant effectivity during deep-sea blowouts, and the development of next-generation oil spill response technologies.

Dr. Amit Patil received his Ph.D. in chemical engineering from the multiphase reactor group at TU Eindhoven in 2014. Since then, he has been a researcher at SINTEF working in the process technology department. His major research interests are surface and colloid chemistry, emulsion technology, particle technology, and CFD.

Dr. Balram Panjwani received his Ph.D. in mechanical engineering from the Norwegian University of Science and Technology (NTNU) in 2010. Since 2010, he has been working as a senior research scientist at SINTEF. His research interests include emulsion characterization, demulsification, turbulence modelling, multiphase flow, and CFD.

Dr. Galina Simonsen received her Ph.D. in chemical engineering from the Norwegian University of Science and Technology (NTNU) in 2011. She then worked as a postdoctoral researcher at NTNU and started at SINTEF Industry in 2020. Her major research interests are nanotechnology, surface and colloid chemistry, emulsion technology, and fluid dynamics.

## ■ ACKNOWLEDGMENTS

The authors thank the The Research Council of Norway (NFR) funded project Improved Separator Design through Dense Packed Layer (DPL) Extraction and Treatment (Grant No. 285590) for financial support.

## ■ REFERENCES

(1) Mozaffari, S.; Tchoukov, P.; Mozaffari, A.; Atias, J.; Czarnecki, J.; Nazemifard, N. Capillary Driven Flow in Nanochannels - Application to Heavy Oil Rheology Studies. *Colloids Surf., A* **2017**, *513*, 178−187.
(2) Fakher, S.; Ahdaya, M.; Elturki, M.; Imqam, A. Critical Review of Asphaltene Properties and Factors Impacting Its Stability in Crude Oil. *J. Pet. Explor. Prod. Technol.* **2020**, *10* (3), 1183−1200.
(3) Speight, J. G. *The Chemistry and Technology of Petroleum*, Fifth ed.; CRC Press, 2014.
(4) Vargas, F. M.; Tavakkoli, M. *Asphaltene Deposition: Fundamentals, Prediction, Prevention, and Remediation*; CRC Press, 2018.
(5) Alimohammadi, S.; Zendehboudi, S.; James, L. A Comprehensive Review of Asphaltene Deposition in Petroleum Reservoirs: Theory, Challenges, and Tips. *Fuel* **2019**, *252*, 753−791.
(6) Drummond, C.; Israelachvili, J. Fundamental Studies of Crude Oil-Surface Water Interactions and Its Relationship to Reservoir Wettability. *J. Pet. Sci. Eng.* **2004**, *45* (1), 61−81.
(7) Struchkov, I. A.; Rogachev, M. K.; Kalinin, E. S.; Roschin, P. V. Laboratory Investigation of Asphaltene-Induced Formation Damage. *J. Pet. Explor. Prod. Technol.* **2019**, *9* (2), 1443−1455.
(8) Syunyaev, R. Z.; Balabin, R. M.; Akhatov, I. S.; Safieva, J. O. Adsorption of Petroleum Asphaltenes onto Reservoir Rock Sands Studied by Near-Infrared (NIR) Spectroscopy. *Energy Fuels* **2009**, *23* (3), 1230−1236.
(9) Al-Hosani, A.; Ravichandran, S.; Daraboina, N. Review of Asphaltene Deposition Modeling in Oil and Gas Production. *Energy Fuels* **2021**, *35* (2), 965−986.
(10) Shoushtari, A. B.; Asadolahpour, S. R.; Madani, M. Thermodynamic Investigation of Asphaltene Precipitation and Deposition Profile in Wellbore: A Case Study. *J. Mol. Liq.* **2020**, *320*, 114468.
(11) Ahooei, A.; Norouzi-Apourvari, S.; Hemmati-Sarapardeh, A.; Schaffie, M. Experimental Study and Modeling of Asphaltene Deposition on Metal Surfaces via Electrodeposition Process: The Role of Ultrasonic Radiation, Asphaltene Concentration and Structure. *J. Pet. Sci. Eng.* **2020**, *195*, 107734.
(12) Mahmoudi Alemi, F.; Mousavi Dehghani, S. A.; Rashidi, A.; Hosseinpour, N.; Mohammadi, S. Synthesize of MWCNT-Fe2O3 Nanocomposite for Controlling Formation and Growth of Asphaltene Particles in Unstable Crude Oil. *Colloids Surf., A* **2021**, *615*, 126295.
(13) Nguele, R.; Sasaki, K. Asphaltene Behavior at the Interface Oil-Nanofluids: Implications to Adsorption. *Colloids Surf., A* **2021**, *622*, 126630.
(14) Korneev, D. S.; Pevneva, G. S.; Voronetskaya, N. G. Effects of the Composition and Molecular Structure of Heavy Oil Asphaltenes on Their Reactivity in Thermal Decomposition Processes. *Pet. Chem.* **2021**, *61* (2), 152−161.
(15) Kamkar, M.; Natale, G. A Review on Novel Applications of Asphaltenes: A Valuable Waste. *Fuel* **2021**, *285*, 119272.
(16) Mullins, O. C. The Asphaltenes. *Annu. Rev. Anal. Chem.* **2011**, *4* (1), 393−418.
(17) Gaweł, B.; Eftekhardadkhah, M.; Øye, G. Elemental Composition and Fourier Transform Infrared Spectroscopy Analysis of Crude Oils and Their Fractions. *Energy Fuels* **2014**, *28* (2), 997−1003.
(18) Rogel, E.; Moir, M.; Witt, M. Atmospheric Pressure Photoionization and Laser Desorption Ionization Coupled to Fourier Transform Ion Cyclotron Resonance Mass Spectrometry To Characterize Asphaltene Solubility Fractions: Studying the Link between Molecular Composition and Physical Behavior. *Energy Fuels* **2015**, *29* (7), 4201−4209.
(19) Hurt, M. R.; Borton, D. J.; Choi, H. J.; Kenttämaa, H. I. Comparison of the Structures of Molecules in Coal and Petroleum Asphaltenes by Using Mass Spectrometry. *Energy Fuels* **2013**, *27* (7), 3653−3658.
(20) Chacón-Patiño, M. L.; Rowland, S. M.; Rodgers, R. P. Advances in Asphaltene Petroleomics. Part 1: Asphaltenes Are Composed of Abundant Island and Archipelago Structural Motifs. *Energy Fuels* **2017**, *31* (12), 13509−13518.
(21) Chacón-Patiño, M. L.; Rowland, S. M.; Rodgers, R. P. Advances in Asphaltene Petroleomics. Part 2: Selective Separation Method That Reveals Fractions Enriched in Island and Archipelago Structural Motifs by Mass Spectrometry. *Energy Fuels* **2018**, *32* (1), 314−328.
(22) Chacón-Patiño, M. L.; Rowland, S. M.; Rodgers, R. P. Advances in Asphaltene Petroleomics. Part 3. Dominance of Island or Archipelago Structural Motif Is Sample Dependent. *Energy Fuels* **2018**, *32* (9), 9106−9120.
(23) Eyssautier, J.; Frot, D.; Barré, L. Structure and Dynamic Properties of Colloidal Asphaltene Aggregates. *Langmuir* **2012**, *28* (33), 11997−12004.
(24) Ekramipooya, A.; Valadi, F. M.; Farisabadi, A.; Gholami, M. R. Effect of the Heteroatom Presence in Different Positions of the Model Asphaltene Structure on the Self-Aggregation: MD and DFT Study. *J. Mol. Liq.* **2021**, *334*, 116109.
(25) Groenzin, H.; Mullins, O. C. Molecular Size and Structure of Asphaltenes from Various Sources. *Energy Fuels* **2000**, *14* (3), 677−684.
(26) Parra-Barraza, H.; Hernández-Montiel, D.; Lizardi, J.; Hernández, J.; Herrera Urbina, R.; Valdez, M. A. The Zeta Potential and Surface Properties of Asphaltenes Obtained with Different Crude Oil/n-Heptane Proportions. *Fuel* **2003**, *82* (8), 869−874.
(27) Dechaine, G. P.; Gray, M. R. Chemistry and Association of Vanadium Compounds in Heavy Oil and Bitumen, and Implications for Their Selective Removal. *Energy Fuels* **2010**, *24* (5), 2795−2808.
(28) Biktagirov, T.; Gafurov, M.; Mamin, G.; Gracheva, I.; Galukhin, A.; Orlinskii, S. In Situ Identification of Various Structural Features of Vanadyl Porphyrins in Crude Oil by High-Field (3.4 T) Electron-Nuclear Double Resonance Spectroscopy Combined with Density Functional Theory Calculations. *Energy Fuels* **2017**, *31* (2), 1243−1249.


https://doi.org/10.1021/acs.energyfuels.1c01990
*Energy Fuels* 2021, 35, 19191−19210

(29) *Structures and Dynamics of Asphaltenes*; Mullins, O. C., Sheu, E. Y., Eds.; Springer: US, 1998. DOI: 10.1007/978-1-4899-1615-0.
(30) Rashid, Z.; Wilfred, C. D.; Gnanasundaram, N.; Arunagiri, A.; Murugesan, T. A Comprehensive Review on the Recent Advances on the Petroleum Asphaltene Aggregation. *J. Pet. Sci. Eng.* **2019**, *176*, 249−268.
(31) Mullins, O. C.; Seifert, D. J.; Zuo, J. Y.; Zeybek, M. Clusters of Asphaltene Nanoaggregates Observed in Oilfield Reservoirs. *Energy Fuels* **2013**, *27* (4), 1752−1761.
(32) Maqbool, T.; Srikiratiwong, P.; Fogler, H. S. Effect of Temperature on the Precipitation Kinetics of Asphaltenes. *Energy Fuels* **2011**, *25* (2), 694−700.
(33) Kar, T.; Hascakir, B. The Role of Resins, Asphaltenes, and Water in Water-Oil Emulsion Breaking with Microwave Heating. *Energy Fuels* **2015**, *29* (6), 3684−3690.
(34) Guzmán, R.; Rodríguez, S.; Torres-Mancera, P.; Ancheyta, J. Evaluation of Asphaltene Stability of a Wide Range of Mexican Crude Oils. *Energy Fuels* **2021**, *35* (1), 408−418.
(35) Derakhshani-Molayousefi, M.; McCullagh, M. Deterring Effect of Resins on the Aggregation of Asphaltenes in N-Heptane. *Energy Fuels* **2020**, *34* (12), 16081−16088.
(36) Rogel, E. Molecular Thermodynamic Approach to the Formation of Mixed Asphaltene-Resin Aggregates. *Energy Fuels* **2008**, *22* (6), 3922−3929.
(37) Gray, M. R.; Tykwinski, R. R.; Stryker, J. M.; Tan, X. Supramolecular Assembly Model for Aggregation of Petroleum Asphaltenes. *Energy Fuels* **2011**, *25* (7), 3125−3134.
(38) Goual, L. Petroleum Asphaltenes. In *Crude Oil Emulsions − Composition Stability and Characterization*; El-Sayed Abdel-Raouf, M., Ed.; InTech, 2012; Chapter 2. DOI: 10.5772/35875.
(39) Goual, L.; Sedghi, M.; Zeng, H.; Mostowfi, F.; McFarlane, R.; Mullins, O. C. On the Formation and Properties of Asphaltene Nanoaggregates and Clusters by DC-Conductivity and Centrifugation. *Fuel* **2011**, *90* (7), 2480−2490.
(40) Adams, J. J. Asphaltene Adsorption, a Literature Review. *Energy Fuels* **2014**, *28* (5), 2831−2856.
(41) Hosseinpour, N.; Khodadadi, A. A.; Bahramian, A.; Mortazavi, Y. Asphaltene Adsorption onto Acidic/Basic Metal Oxide Nanoparticles toward in Situ Upgrading of Reservoir Oils by Nanotechnology. *Langmuir* **2013**, *29* (46), 14135−14146.
(42) A Issaka, S. Review on the Fundamental Aspects of Petroleum Oil Emulsions and Techniques of Demulsification. *J. Pet. Environ. Biotechnol.* **2015**, *06* (02), na DOI: 10.4172/2157-7463.1000214.
(43) Zolfaghari, R.; Fakhru'l-Razi, A.; Abdullah, L. C.; Elnashaie, S. S. E. H.; Pendashteh, A. Demulsification Techniques of Water-in-Oil and Oil-in-Water Emulsions in Petroleum Industry. *Sep. Purif. Technol.* **2016**, *170*, 377−407.
(44) Mohammed, S. A. M.; Mohammed, M. S. The Application of Microwave Technology in Demulsification of Water-in-Oil Emulsion for Missan Oil Fields. *Iraqi Journal of Chemical and Petroleum Engineering* **2013**, *14* (2), 21−27.
(45) Umar, A. A.; Saaid, I. B. M.; Sulaimon, A. A.; Pilus, R. B. M. A Review of Petroleum Emulsions and Recent Progress on Water-in-Crude Oil Emulsions Stabilized by Natural Surfactants and Solids. *J. Pet. Sci. Eng.* **2018**, *165*, 673−690.
(46) Piroozian, A.; Hemmati, M.; Safari, M.; Rahimi, A.; Rahmani, O.; Aminpour, S. M.; Pour, A. B. A Mechanistic Understanding of the Water-in-Heavy Oil Emulsion Viscosity Variation: Effect of Asphaltene and Wax Migration. *Colloids Surf., A* **2021**, *608*, 125604.
(47) Patil, A.; Arnesen, K.; Holte, A.; Farooq, U.; Brunsvik, A.; Størseth, T.; Johansen, S. T. Crude Oil Characterization with a New Dynamic Emulsion Stability Technique. *Fuel* **2021**, *290*, 120070.
(48) Kokal, S. L. Crude Oil Emulsions: A State-Of-The-Art Review. *SPE Prod. Facil.* **2005**, *20* (01), 5−13.
(49) Kilpatrick, P. K. Water-in-Crude Oil Emulsion Stabilization: Review and Unanswered Questions. *Energy Fuels* **2012**, *26* (7), 4017−4026.
(50) Fan, Y.; Simon, S.; Sjöblom, J. Interfacial Shear Rheology of Asphaltenes at Oil-Water Interface and Its Relation to Emulsion Stability: Influence of Concentration, Solvent Aromaticity and Nonionic Surfactant. *Colloids Surf., A* **2010**, *366* (1), 120−128.
(51) Maiti, S.; Mishra, I. M.; Bhattacharya, S. D.; Joshi, J. K. Removal of Oil from Oil-in-Water Emulsion Using a Packed Bed of Commercial Resin. *Colloids Surf., A* **2011**, *389* (1), 291−298.
(52) Yi, M.; Huang, J.; Wang, L. Research on Crude Oil Demulsification Using the Combined Method of Ultrasound and Chemical Demulsifier. *J. Chem.* **2017**, *2017*, 1.
(53) Carneiro, G. F.; Silva, R. C.; Barbosa, L. L.; Freitas, J. C. C.; Sad, C. M. S.; Tose, L. V.; Vaz, B. G.; Romão, W.; de Castro, E. V. R.; Neto, A. C.; Lacerda, V. Characterisation and Selection of Demulsifiers for Water-in-Crude Oil Emulsions Using Low-Field 1H NMR and ESI-FT-ICR MS. *Fuel* **2015**, *140*, 762−769.
(54) Mhatre, S.; Simon, S.; Sjöblom, J.; Xu, Z. Demulsifier Assisted Film Thinning and Coalescence in Crude Oil Emulsions under DC Electric Fields. *Chem. Eng. Res. Des.* **2018**, *134*, 117−129.
(55) Vennela, N.; Mondal, S.; De, S.; Bhattacharjee, S. Sherwood Number in Flow through Parallel Porous Plates (Microchannel) Due to Pressure and Electroosmotic Flow. *AIChE J.* **2012**, *58* (6), 1693−1703.
(56) Fan, G.; Lyu, R.; Gao, X.; Liang, C.; Wang, C. MPEG Grafted Quaternized Carboxymethyl Chitosan for Demulsification of Crude Oil Emulsions: ARTICLE. *J. Appl. Polym. Sci.* **2018**, *135* (7), 45867.
(57) Sun, N.; Jiang, H.; Wang, Y.; Qi, A. A Comparative Research of Microwave, Conventional-Heating, and Microwave/Chemical Demulsification of Tahe Heavy-Oil-in-Water Emulsion. *SPE Prod. Oper.* **2018**, *33* (02), 371−381.
(58) Wen, Y.; Cheng, H.; Lu, L.-J.; Liu, J.; Feng, Y.; Guan, W.; Zhou, Q.; Huang, X.-F. Analysis of Biological Demulsification Process of Water-in-Oil Emulsion by Alcaligenes Sp. S-XJ-1. *Bioresour. Technol.* **2010**, *101* (21), 8315−8322.
(59) Nikkhah, M.; Tohidian, T.; Rahimpour, M. R.; Jahanmiri, A. Efficient Demulsification of Water-in-Oil Emulsion by a Novel Nano-Titania Modified Chemical Demulsifier. *Chem. Eng. Res. Des.* **2015**, *94*, 164−172.
(60) Ali, N.; Zhang, B.; Zhang, H.; Zaman, W.; Li, X.; Li, W.; Zhang, Q. Interfacially Active and Magnetically Responsive Composite Nanoparticles with Raspberry like Structure; Synthesis and Its Applications for Heavy Crude Oil/Water Separation. *Colloids Surf., A* **2015**, *472*, 38−49.
(61) Razi, M.; Rahimpour, M. R.; Jahanmiri, A.; Azad, F. Effect of a Different Formulation of Demulsifiers on the Efficiency of Chemical Demulsification of Heavy Crude Oil. *J. Chem. Eng. Data* **2011**, *56* (6), 2936−2945.
(62) Daniel-David, D.; Le Follotec, A.; Pezron, I.; Dalmazzone, C.; Noïk, C.; Barré, L.; Komunjer, L. Destabilisation of Water-in-Crude Oil Emulsions by Silicone Copolymer Demulsifiers. *Oil Gas Sci. Technol.* **2008**, *63* (1), 165−173.
(63) Shehzad, F.; Hussein, I. A.; Kamal, M. S.; Ahmad, W.; Sultan, A. S.; Nasser, M. S. Polymeric Surfactants and Emerging Alternatives Used in the Demulsification of Produced Water: A Review. *Polym. Rev.* **2018**, *58* (1), 63−101.
(64) Simonsen, G.; Strand, M.; Øye, G. Potential Applications of Magnetic Nanoparticles within Separation in the Petroleum Industry. *J. Pet. Sci. Eng.* **2018**, *165*, 488−495.
(65) Ko, S.; Kim, E. S.; Park, S.; Daigle, H.; Milner, T. E.; Huh, C.; Bennetzen, M. V.; Geremia, G. A. Oil Droplet Removal from Produced Water Using Nanoparticles and Their Magnetic Separation. In *SPE Annual Technical Conference and Exhibition*; Society of Petroleum Engineers: Dubai, UAE, 2016. DOI: 10.2118/181893-MS.
(66) Wang, X.; Shi, Y.; Graff, R. W.; Lee, D.; Gao, H. Developing Recyclable PH-Responsive Magnetic Nanoparticles for Oil-Water Separation. *Polymer* **2015**, *72*, 361−367.
(67) Józefczak, A.; Wlazło, R. Ultrasonic Studies of Emulsion Stability in the Presence of Magnetic Nanoparticles. *Adv. Condens. Matter Phys.* **2015**, *2015*, 1.
(68) Nassar, N. N. Asphaltene Adsorption onto Alumina Nanoparticles: Kinetics and Thermodynamic Studies. *Energy Fuels* **2010**, *24* (8), 4116−4122.

(69) Tayakout, M.; Ferreira, C.; Espinat, D.; Arribas Picon, S.; Sorbier, L.; Guillaume, D.; Guibard, I. Diffusion of Asphaltene Molecules through the Pore Structure of Hydroconversion Catalysts. *Chem. Eng. Sci.* **2010**, *65* (5), 1571−1583.
(70) Mansoori Mosleh, F.; Mortazavi, Y.; Hosseinpour, N.; Khodadadi, A. A. Asphaltene Adsorption onto Carbonaceous Nanostructures. *Energy Fuels* **2020**, *34* (1), 211−224.
(71) Vargas, V.; Castillo, J.; Ocampo-Torres, R.; Lienemann, C.-P.; Bouyssiere, B. Surface Modification of SiO2 Nanoparticles to Increase Asphaltene Adsorption. *Pet. Sci. Technol.* **2018**, *36* (8), 618−624.
(72) Guzmán, J. D.; Betancur, S.; Carrasco-Marín, F.; Franco, C. A.; Nassar, N. N.; Cortés, F. B. Importance of the Adsorption Method Used for Obtaining the Nanoparticle Dosage for Asphaltene-Related Treatments. *Energy Fuels* **2016**, *30* (3), 2052−2059.
(73) Nassar, N. N.; Hassan, A.; Carbognani, L.; Lopez-Linares, F.; Pereira-Almao, P. Iron Oxide Nanoparticles for Rapid Adsorption and Enhanced Catalytic Oxidation of Thermally Cracked Asphaltenes. *Fuel* **2012**, *95*, 257−262.
(74) Nassar, N. N.; Hassan, A.; Pereira-Almao, P. Metal Oxide Nanoparticles for Asphaltene Adsorption and Oxidation. *Energy Fuels* **2011**, *25*, 1017−1023.
(75) Nassar, N. N.; Hassan, A.; Pereira-Almao, P. Comparative Oxidation of Adsorbed Asphaltenes onto Transition Metal Oxide Nanoparticles. *Colloids Surf., A* **2011**, *384* (1), 145−149.
(76) Betancur, S.; Carmona, J. C.; Nassar, N. N.; Franco, C. A.; Cortés, F. B. Role of Particle Size and Surface Acidity of Silica Gel Nanoparticles in Inhibition of Formation Damage by Asphaltene in Oil Reservoirs. *Ind. Eng. Chem. Res.* **2016**, *55* (21), 6122−6132.
(77) Taborda, E. A.; Franco, C. A.; Lopera, S. H.; Alvarado, V.; Cortés, F. B. Effect of Nanoparticles/Nanofluids on the Rheology of Heavy Crude Oil and Its Mobility on Porous Media at Reservoir Conditions. *Fuel* **2016**, *184*, 222−232.
(78) Shayan, N. N.; Mirzayi, B. Adsorption and Removal of Asphaltene Using Synthesized Maghemite and Hematite Nanoparticles. *Energy Fuels* **2015**, *29*, 1397−1406.
(79) Mirzayi, B.; Shayan, N. N. Adsorption Kinetics and Catalytic Oxidation of Asphaltene on Synthesized Maghemite Nanoparticles. *J. Pet. Sci. Eng.* **2014**, *121*, 134−141.
(80) Kashefi, S.; Lotfollahi, M. N.; Shahrabadi, A. Investigation of Asphaltene Adsorption onto Zeolite Beta Nanoparticles to Reduce Asphaltene Deposition in a Silica Sand Pack. *Oil Gas Sci. Technol.* **2018**, *73*, 2.
(81) Farooq, U.; Nourani, M.; Ivol, F.; Årrestad, A. B.; Øye, G. Adsorption of Crude Oil Components on Mineral Surfaces Followed by Quartz Crystal Microbalance and Contact Angle Measurements: The Effect of Oil Composition, Simulated Weathering and Dispersants. *Energy Fuels* **2019**, *33* (3), 2359−2365.
(82) Al-Jabari, M.; Nassar, N.; Husien, M. Separation of Asphaltenes from Heavy Oil Model-Solutions by Adsorption on Colloidal Magnetite Nanoparticles. In *ICCE-2007 Conference*, Kuwait, 2007.
(83) Olaitan, A. D.; Reyes, K. A.; Barnes, L. F.; Yount, J. R.; Ward, S.; Hamilton, H. S. C.; King, K. E.; Van Leeuwen, C. J.; Stepherson, J. R.; Vargas, T. k.; Kirkconnell, M. P.; Molek, K. S. Transition Metal Oxide Nanoparticles as Surfaces for Surface-Assisted Laser Desorption/Ionization Mass Spectrometry of Asphaltenes. *Pet. Sci. Technol.* **2017**, *35* (19), 1917−1924.
(84) Madhi, M.; Bemani, A.; Daryasafar, A.; Khosravi Nikou, M. R. Experimental and Modeling Studies of the Effects of Different Nanoparticles on Asphaltene Adsorption. *Pet. Sci. Technol.* **2017**, *35* (3), 242−248.
(85) Nassar, N. N.; Hassan, A.; Pereira-Almao, P. Effect of the Particle Size on Asphaltene Adsorption and Catalytic Oxidation onto Alumina Particles. *Energy Fuels* **2011**, *25* (9), 3961−3965.
(86) Cortés, F. B.; Montoya, T.; Acevedo, S.; Nassar, N.; Franco, C. A. Adsorption-Desorption of n-C7 Asphaltenes over Micro- and Nanoparticles of Silica and Its Impact on Wettability Alteration. *CT&F, Cienc., Tecnol. Futuro* **2016**, *6* (4), 89−106.
(87) Abu Tarboush, B. J.; Husein, M. M. Adsorption of Asphaltenes from Heavy Oil onto in Situ Prepared NiO Nanoparticles. *J. Colloid Interface Sci.* **2012**, *378* (1), 64−69.
(88) Abu Tarboush, B. J.; Husein, M. M. Dispersed Fe2O3 Nanoparticles Preparation in Heavy Oil and Their Uptake of Asphaltenes. *Fuel Process. Technol.* **2015**, *133*, 120−127.
(89) Nassar, N. N.; Hassan, A.; Vitale, G. Comparing Kinetics and Mechanism of Adsorption and Thermo-Oxidative Decomposition of Athabasca Asphaltenes onto TiO2, ZrO2, and CeO2 Nanoparticles. *Appl. Catal., A* **2014**, *484*, 161−171.
(90) Nassar, N. N.; Hassan, A.; Pereira-Almao, P. Effect of Surface Acidity and Basicity of Aluminas on Asphaltene Adsorption and Oxidation. *J. Colloid Interface Sci.* **2011**, *360* (1), 233−238.
(91) Adams, J. J. Asphaltene Adsorption, a Literature Review. *Energy Fuels* **2014**, *28* (5), 2831−2856.
(92) Mohammadi, M.; Akbari, M.; Fakhroueian, Z.; Bahramian, A.; Azin, R.; Arya, S. Inhibition of Asphaltene Precipitation by TiO2, SiO2, and ZrO2 Nanofluids. *Energy Fuels* **2011**, *25* (7), 3150−3156.
(93) Nassar, N. N.; Husein, M. M. Ultradispersed Particles in Heavy Oil: Part I, Preparation and Stabilization of Iron Oxide/Hydroxide. *Fuel Process. Technol.* **2010**, *91* (2), 164−168.
(94) Nassar, N. N.; Montoya, T.; Franco, C. A.; Cortés, F. B.; Pereira-Almao, P. A New Model for Describing the Adsorption of Asphaltenes on Porous Media at a High Pressure and Temperature under Flow Conditions. *Energy Fuels* **2015**, *29* (7), 4210−4221.
(95) Cortés, F. B.; Mejía, J. M.; Ruiz, M. A.; Benjumea, P.; Riffel, D. B. Sorption of Asphaltenes onto Nanoparticles of Nickel Oxide Supported on Nanoparticulated Silica Gel. *Energy Fuels* **2012**, *26* (3), 1725−1730.
(96) Franco, C. A.; Nassar, N. N.; Ruiz, M. A.; Pereira-Almao, P.; Cortés, F. B. Nanoparticles for Inhibition of Asphaltenes Damage: Adsorption Study and Displacement Test on Porous Media. *Energy Fuels* **2013**, *27* (6), 2899−2907.
(97) Franco, C.; Patiño, E.; Benjumea, P.; Ruiz, M. A.; Cortés, F. B. Kinetic and Thermodynamic Equilibrium of Asphaltenes Sorption onto Nanoparticles of Nickel Oxide Supported on Nanoparticulated Alumina. *Fuel* **2013**, *105*, 408−414.
(98) Franco, C. A.; Montoya, T.; Nassar, N. N.; Pereira-Almao, P.; Cortés, F. B. Adsorption and Subsequent Oxidation of Colombian Asphaltenes onto Nickel and/or Palladium Oxide Supported on Fumed Silica Nanoparticles. *Energy Fuels* **2013**, *27* (12), 7336−7347.
(99) Panahi, S.; Sardarian, A. R.; Esmaeilzadeh, F.; Mowla, D. Synthesize and Characterization of Chitosan and Silica Supported on $Fe_3O_4$ Nanoparticles for the Adsorption and Removal of Asphaltene Molecules from Crude Oil. *Mater. Res. Express* **2018**, *5* (9), 095022.
(100) Skartlien, R.; Simon, S.; Sjöblom, J. DPD Molecular Simulations of Asphaltene Adsorption on Hydrophilic Substrates: Effects of Polar Groups and Solubility. *J. Dispersion Sci. Technol.* **2016**, *37* (6), 866−883.
(101) Setoodeh, N.; Darvishi, P.; Esmaeilzadeh, F. Adsorption of Asphaltene from Crude Oil by Applying Polythiophene Coating on Fe3O4 Nanoparticles. *J. Dispersion Sci. Technol.* **2018**, *39* (4), 578−588.
(102) Setoodeh, N.; Darvishi, P.; Lashanizadegan, A. A Comparative Study to Evaluate the Performance of Coated Fe3O4 Nanoparticles for Adsorption of Asphaltene from Crude Oil in Bench Scale. *J. Dispersion Sci. Technol.* **2018**, *39* (5), 711−720.
(103) Peng, J.; Liu, Q.; Xu, Z.; Masliyah, J. Novel Magnetic Demulsifier for Water Removal from Diluted Bitumen Emulsion. *Energy Fuels* **2012**, *26* (5), 2705−2710.
(104) Peng, J.; Liu, Q.; Xu, Z.; Masliyah, J. Synthesis of Interfacially Active and Magnetically Responsive Nanoparticles for Multiphase Separation Applications. *Adv. Funct. Mater.* **2012**, *22* (8), 1732−1740.
(105) He, X.; Liang, C.; Liu, Q.; Xu, Z. Magnetically Responsive Janus Nanoparticles Synthesized Using Cellulosic Materials for Enhanced Phase Separation in Oily Wastewaters and Water-in-Crude Oil Emulsions. *Chem. Eng. J.* **2019**, *378*, 122045.


https://doi.org/10.1021/acs.energyfuels.1c01990
*Energy Fuels* 2021, 35, 19191−19210

(106) Liang, J.; Du, N.; Song, S.; Hou, W. Magnetic Demulsification of Diluted Crude Oil-in-Water Nanoemulsions Using Oleic Acid-Coated Magnetite Nanoparticles. *Colloids Surf., A* **2015**, *466*, 197.
(107) Lan, Q.; Liu, C.; Yang, F.; Liu, S.; Xu, J.; Sun, D. Synthesis of Bilayer Oleic Acid-Coated Fe3O4 Nanoparticles and Their Application in PH-Responsive Pickering Emulsions. *J. Colloid Interface Sci.* **2007**, *310* (1), 260−269.
(108) Liang, C.; He, X.; Liu, Q.; Xu, Z. Adsorption-Based Synthesis of Magnetically Responsive and Interfacially Active Composite Nanoparticles for Dewatering of Water-in-Diluted Bitumen Emulsions. *Energy Fuels* **2018**, *32* (8), 8078−8089.
(109) Chen, Y.; Lin, X.; Liu, N.; Cao, Y.; Lu, F.; Xu, L.; Feng, L. Magnetically Recoverable Efficient Demulsifier for Water-in-Oil Emulsions. *ChemPhysChem* **2015**, *16* (3), 595−600.
(110) Ali, N.; Zhang, Q. Y.; Zhang, B. L.; Zaman, W.; Ali, S. Interfacial and Demulsification Properties of Janus Type Magnetic Nanoparticles. *Adv. Mater. Res.* **2015**, *1105*, 264−268.
(111) Farrokhi, F.; Jafari Nasr, M. R.; Rahimpour, M. R.; Arjmand, M.; Vaziri, S. A. Application of a Novel Magnetic Nanoparticle as Demulsifier for Dewatering in Crude Oil Emulsion. *Sep. Sci. Technol.* **2018**, *53* (3), 551−558.
(112) Xu, H.; Jia, W.; Ren, S.; Wang, J. Novel and Recyclable Demulsifier of Expanded Perlite Grafted by Magnetic Nanoparticles for Oil Separation from Emulsified Oil Wastewaters. *Chem. Eng. J.* **2018**, *337*, 10−18.
(113) Alam, S. N.; Sharma, N.; Kumar, L. Synthesis of Graphene Oxide (GO) by Modified Hummers Method and Its Thermal Reduction to Obtain Reduced Graphene Oxide (RGO)*. *Graphene* **2017**, *06* (1), 1−18.
(114) Menzel, R.; Iruretagoyena, D.; Wang, Y.; Bawaked, S. M.; Mokhtar, M.; Al-Thabaiti, S. A.; Basahel, S. N.; Shaffer, M. S. P. Graphene Oxide/Mixed Metal Oxide Hybrid Materials for Enhanced Adsorption Desulfurization of Liquid Hydrocarbon Fuels. *Fuel* **2016**, *181*, 531−536.
(115) Ancheyta, J.; Sánchez, S.; Rodríguez, M. A. Kinetic Modeling of Hydrocracking of Heavy Oil Fractions: A Review. *Catal. Today* **2005**, *109* (1), 76−92.
(116) Zhang, Z.; Schniepp, H. C.; Adamson, D. H. Characterization of Graphene Oxide: Variations in Reported Approaches. *Carbon* **2019**, *154*, 510−521.
(117) Javadian, S.; Khalilifard, M.; Sadrpoor, S. M. Functionalized Graphene Oxide with Core-Shell of Fe3O4@oliec Acid Nanospheres as a Recyclable Demulsifier for Effective Removal of Emulsified Oil from Oily Wastewater. *Journal of Water Process Engineering* **2019**, *32*, 100961.
(118) Kim, F.; Cote, L. J.; Huang, J. Graphene Oxide: Surface Activity and Two-Dimensional Assembly. *Adv. Mater.* **2010**, *22* (17), 1954−1958.
(119) Liu, J.; Li, X.; Jia, W.; Li, Z.; Zhao, Y.; Ren, S. Demulsification of Crude Oil-in-Water Emulsions Driven by Graphene Oxide Nanosheets. *Energy Fuels* **2015**, *29* (7), 4644−4653.
(120) Fang, S.; Chen, T.; Wang, R.; Xiong, Y.; Chen, B.; Duan, M. Assembly of Graphene Oxide at the Crude Oil/Water Interface: A New Approach to Efficient Demulsification. *Energy Fuels* **2016**, *30* (4), 3355−3364.
(121) Wang, H.; Liu, J.; Xu, H.; Ma, Z.; Jia, W.; Ren, S. Demulsification of Heavy Oil-in-Water Emulsions by Reduced Graphene Oxide Nanosheets. *RSC Adv.* **2016**, *6* (108), 106297−106307.
(122) Contreras Ortiz, S. N.; Cabanzo, R.; Mejía-Ospino, E. Crude Oil/Water Emulsion Separation Using Graphene Oxide and Amine-Modified Graphene Oxide Particles. *Fuel* **2019**, *240*, 162−168.
(123) Liu, J.; Wang, H.; Li, X.; Jia, W.; Zhao, Y.; Ren, S. Recyclable Magnetic Graphene Oxide for Rapid and Efficient Demulsification of Crude Oil-in-Water Emulsion. *Fuel* **2017**, *189*, 79−87.
(124) Javadian, S.; Sadrpoor, S. M. Demulsification of Water in Oil Emulsion by Surface Modified SiO2 Nanoparticle. *J. Pet. Sci. Eng.* **2020**, *184*, 106547.
(125) Yegya Raman, A. K.; Aichele, C. P. Demulsification of Surfactant-Stabilized Water-in-Oil (Cyclohexane) Emulsions Using Silica Nanoparticles. *Energy Fuels* **2018**, *32* (8), 8121−8130.
(126) Hassan, S. A.; Abdalla, B. K.; Mustafa, M. A. Addition of Silica Nano-Particles for the Enhancement of Crude Oil Demulsification Process. *Pet. Sci. Technol.* **2019**, *37* (13), 1603−1611.
(127) Qi, L.; Song, C.; Wang, T.; Li, Q.; Hirasaki, G. J.; Verduzco, R. Polymer-Coated Nanoparticles for Reversible Emulsification and Recovery of Heavy Oil. *Langmuir* **2018**, *34* (22), 6522−6528.
(128) Gandomkar, G. E.; Bekhradinassab, E.; Sabbaghi, S.; Zerafat, M. M. Improvement of Chemical Demulsifier Performance Using Silica Nanoparticles. *Int. J. of Chem. and Mol. Eng.* **2016**, *9* (4), 585−588.
(129) Fang-Hui, W.; Hong, Z. The Application and Research of Dispersing In Situ Nano-SiO2 in Polyether Demulsifier TA1031. *J. Dispersion Sci. Technol.* **2008**, *29* (8), 1081−1084.
(130) Wang, F. H.; Shen, L. B.; Zhu, H.; Han, K. F. The Preparation of a Polyether Demulsifier Modified by Nano-SiO2 and the Effect on Asphaltenes and Resins. *Pet. Sci. Technol.* **2011**, *29* (24), 2521−2529.
(131) Wang, H.; Xu, H.; Jia, W.; Ren, S. Functionalized Carbon Black Nanoparticles Used for Separation of Emulsified Oil from Oily Wastewater. *J. Dispersion Sci. Technol.* **2018**, *39* (4), 497−506.
(132) Ye, F.; Jiang, X.; Mi, Y.; Kuang, J.; Huang, Z.; Yu, F.; Zhang, Z.; Yuan, H. Preparation of Oxidized Carbon Black Grafted with Nanoscale Silica and Its Demulsification Performance in Water-in-Oil Emulsion. *Colloids Surf., A* **2019**, *582*, 123878.
(133) Xu, H.; Jia, W.; Ren, S.; Wang, J. Magnetically Responsive Multi-Wall Carbon Nanotubes as Recyclable Demulsifier for Oil Removal from Crude Oil-in-Water Emulsion with Different PH Levels. *Carbon* **2019**, *145*, 229−239.
(134) Huang, Z.; Li, P.; Luo, X.; Jiang, X.; Liu, L.; Ye, F.; Kuang, J.; Luo, Y.; Mi, Y. Synthesis of a Novel Environmentally Friendly and Interfacially Active CNTs/SiO2 Demulsifier for W/O Crude Oil Emulsion Separation. *Energy Fuels* **2019**, *33* (8), 7166−7175.
(135) Franco, C. A.; Nassar, N. N.; Cortés, F. B. Removal of Oil from Oil-in-Saltwater Emulsions by Adsorption onto Nano-Alumina Functionalized with Petroleum Vacuum Residue. *J. Colloid Interface Sci.* **2014**, *433*, 58−67.
(136) Ko, S.; Prigiobbe, V.; Huh, C.; Bryant, S. L.; Bennetzen, M. V.; Mogensen, K. Accelerated Oil Droplet Separation from Produced Water Using Magnetic Nanoparticles. In *SPE Annual Technical Conference and Exhibition*; Society of Petroleum Engineers: Amsterdam, The Netherlands, 2014. DOI: 10.2118/170828-MS.
(137) Mirshahghassemi, S.; Lead, J. R. Oil Recovery from Water under Environmentally Relevant Conditions Using Magnetic Nanoparticles. *Environ. Sci. Technol.* **2015**, *49* (19), 11729−11736.
(138) Palchoudhury, S.; Lead, J. R. A Facile and Cost-Effective Method for Separation of Oil-Water Mixtures Using Polymer-Coated Iron Oxide Nanoparticles. *Environ. Sci. Technol.* **2014**, *48* (24), 14558−14563.
(139) Lü, T.; Zhang, S.; Qi, D.; Zhang, D.; Vance, G. F.; Zhao, H. Synthesis of PH-Sensitive and Recyclable Magnetic Nanoparticles for Efficient Separation of Emulsified Oil from Aqueous Environments. *Appl. Surf. Sci.* **2017**, *396*, 1604−1612.
(140) Zhou, J.; Chang, Q.; Wang, Y.; Wang, J.; Meng, G. Separation of Stable Oil-Water Emulsion by the Hydrophilic Nano-Sized ZrO2Modified Al2O3Microfiltration Membrane. *Sep. Purif. Technol.* **2010**, *75* (3), 243−248.
(141) Gandomkar, G. E.; Bekhradinassab, E.; Sabbaghi, S.; Zerafat, M. M. Improvement of Chemical Demulsifier Performance Using Silica Nanoparticles. *Int. J. Chem. Mol. Eng.* **2016**, *9* (4), 585−588.